O3M SAF ORR VALIDATION REPORT

Validated products:

Identifier	Name	Acronym
O3M-176	NRT Total HCHO	MAG-N-HCHO
O3M-177	from GOME-2A & B	MBG-N-HCHO
O3M-10	Offline Total HCHO	MAG-O-HCHO
O3M-58	from GOME-2A & B	MAG-O-HCHO
O3M-118	Reprocessed Total HCHO from GOME-2A & B	MxG-RP1-HCHO

Authors:

Name	Institute
Isabelle De Smedt	Belgian Institute for Space Aeronomy
Gaia Pinardi	Belgian Institute for Space Aeronomy
Huan Yu	Belgian Institute for Space Aeronomy
François Hendrick	Belgian Institute for Space Aeronomy
Clio Gielen	Belgian Institute for Space Aeronomy
Nan Hao	German Aerospace Center
Mathias Begoin	German Aerospace Center
Pieter Valks	German Aerospace Center

Reporting period: for GOME-2/MetOp-A, January 2007 – July 2015

for GOME-2/MetOp-B, January 2013 – July 2015

Input data versions: GOME-2 Level 1B version 5.3.0 until 17 June 2014

GOME-2 Level 1B version 6.0.0 since 17 June 2014

Data processor versions: GDP 4.8, UPAS version 1.3.9

authors I. De Smedt, G. Pinardi, H. Yu, F. Hendrick, C. Gielen, N. Hao, M. Begoin and P. Valks

edited by I. De Smedt, BIRA-IASB, Brussels, Belgium

reference SAF/O3M/IASB/VR/HCHO/113/TN-IASB-GOME2-O3MSAF-HCHO-2015

document type O3M-SAF Validation Report
issue 1

revision *1*
date of issue 31 October 2015
products MAG-N-HCHO MBG-N-HCHO MAG-O-HCHO MBG-O-HCHO MxG-RP1-HCHO
identifier O3M-176, -177, -10, -58 and -118
product version level-0-to-1 v5.3 and 6.0, level-1-to-2 GDP v4.8

distribution / *distribution*

Function	***Organisation***
O3M-SAF	EUMETSAT, BIRA-IASB, DLR, DMI, DWD, FMI, HNMS/AUTH, KNMI, LATMOS, RMI

external contributors / *contributions externes au SAF*

contributing ground-based correlative measurements

Acronym	***Organisation***	***Country***
BIRA-IASB	Belgian Institute for Space Aeronomy	Belgium

document change record / *historique du document*

Issue	***Rev.***	***Date***	***Section***	***Description of Change***
1	0	31.07.2015	all	Creation of this document

Validation report of GOME-2 NRT, offline and reprocessed GDP 4.8 HCHO column data for MetOp-A and B

CONTENTS

ACRONYMS AND ABBREVIATIONS

AMF	Air Mass Factor, or optical enhancement factor
BIRA-IASB	Belgian Institute for Space Aeronomy
DLR	German Aerospace Centre
DOAS	Differential Optical Absorption Spectroscopy
Envisat	Environmental Satellite
ESA	European Space Agency
EUMETSAT	European Organisation for the Exploitation of Meteorological Satellites
GDP	GOME Data Processor
GOME	Global Ozone Monitoring Experiment
IMF	Remote Sensing Technology Institute
LOS	Line Of Sight
NDACC	Network for the Detection of Atmospheric Composition Change
HCHO	Formaldehyde
O_3	Ozone
O3M-SAF	Ozone and Atmospheric Chemistry Monitoring Satellite Application Facility
OCRA	Optical Cloud Recognition Algorithm
OMI	Ozone Monitoring Instrument
ROCINN	Retrieval of Cloud Information using Neural Networks
RRS	Rotational Raman Scattering
RTS	RT Solutions Inc.
SCD	Slant Column Density
SCIAMACHY	Scanning Imaging Absorption spectroMeter for Atmospheric CHartography
SNR	Signal to Noise Ratio
SZA	Solar Zenith Angle
TEMIS	Tropospheric Emission Monitoring Internet Service
UPAS	Universal Processor for UV/VIS Atmospheric Spectrometers
UVVIS	Ultraviolet-visible spectrometry
VCD	Vertical Column Density
WMO	World Meteorological Organization

DATA DESCRIPTION FOR THE METOP-A AND B GOME-2 TOTAL HCHO DATA PRODUCTS

In the framework of EUMETSAT's Satellite Application Facility on Ozone and Atmospheric Chemistry Monitoring (O3M-SAF), GOME-2 formaldehyde (HCHO) total column data product, as well as associated cloud parameters, are delivered in NRT and off-line. Those data products are generated at DLR from GOME-2 measurements using the UPAS environment version 1.3.9, the level-0-to-1 v5.3 and v6.0 processors and the level-1-to-2 GDP v4.8 DOAS retrieval processor (see [ATBD] and [PUM]). BIRA-IASB and DLR ensure detailed quality assessment of algorithm upgrades and continuous monitoring of GOME-2 HCHO data quality with a recurring geophysical validation using correlative measurements from independent retrievals, from other satellites and from ground-based instruments and modelling support.

This report presents the validation of the NRT, offline and reprocessed MetOp-A and B GOME-2 HCHO column data retrieved using the new version 4.8 of the level-1-to-2 GDP vs DOAS retrieval processor. In the following, the abbreviations GOME-2A and GOME-2B are used as short names for MetOp-A GOME-2 and MetOp-B GOME-2. When used alone, the terms MetOp or GOME-2 stand for MetOp-A and MetOp-B, or GOME-2A and GOME-2B.

SUMMARY

The main results from the verification are summarized hereafter:

- The new version 4.8 of the GDP processor includes a number of improvements proposed by BIRA-IASB in the previous ORR reports (O3-SAF, 2013).
- Improvement of the HCHO product has been obtained, both for GOME-2 on MetOp-A and MetOp-B. In particular, a significant reduction of the noise on the slant columns has been obtained by using two fitting intervals.
- The current quality of the MetOp GOME-2 radiance and irradiance spectra in the 328.5-346 nm and 332-359 nm spectral intervals enables stable DOAS retrievals.
- GOME-2B HCHO corrected slant columns, fit residuals, and scatters are comparable to those obtained from GOME-2A spectra in 2007, both for the UPAS and the scientific products. However, GOME-2B HCHO (uncorrected) slant columns present larger offsets than GOME-2A in 2007.
- The degradation of GOME-2A spectra along the years tends to increase the negative offsets of HCHO (uncorrected) slant columns, both in the UPAS and the scientific products. However, in the scientific algorithm, the use of remote radiance spectra instead of solar irradiance as background in the DOAS equation allows for a reduction of the offsets. The background radiance spectra are selected daily in the remote Equatorial Pacific region.
- Ultimately, the offsets in slant columns are efficiently corrected by the reference sector correction, both in the UPAS and the scientific products.
- A remaining cause of differences between GDP 4.8 and the scientific product is the introduction of O_4 as absorbing cross-sections in the fits. While O_4 absorption can be fitted by the polynomial in the small interval (328.5-346), it is not the case anymore in the large interval (328.5-359). It is our recommendation to include this cross-section in both intervals.
- Further improvement of the slant column fits could be obtained by including O_4 as absorber in the fits in both intervals (HCHO SCD in Africa), by using remote radiance spectra as reference in the DOAS equation (HCHO SCD offsets), by fitting the instrumental slit function during the Fraunhofer wavelength calibration (RMS degradation), and by implementing an iterative spike removal algorithm (fit quality in the South Atlantic Anomaly).
- Differences between the operational and scientific HCHO vertical columns are well understood and related to the different input parameters used for the air mass factor calculation, namely the cloud product (cloud top pressure, cloud albedo, and cloud fraction) and the surface albedo, as already reported in the validation report of GOME-2A GDP 4.4 HCHO (O3-SAF validation Report, 2010).
- The cloud product used in the operational product has been improved. The cloud-corrected and clear-sky AMFs are in better agreement, no systematic bias is observed. The GOME-2A degradation effects on the cloud product have been greatly reduced in GDP 4.8.
- A major improvement of the operational product is the provision of the averaging kernels in the HCHO operational product.
- Validation of the operational HCHO product using correlative ground-based MAX-DOAS columns and profiles in Xianghe, Brussels and Bujumbura are very satisfactory. The smoothed columns generally agree within 3 to 13%, with the exeption of GOME-2B in Bujumbura where satellite columns are 38% higher than MAX-DOAS.

A. INTRODUCTION

A.1. Scope of this document

The present document reports on the validation of NRT, offline and reprocessed GOME-2 HCHO column data acquired using the new version 4.8 of GOME Data Processor (GDP) operated at the DLR Remote Sensing Technology Institute (DLR-IMF, Oberpfaffenhofen, Germany) in the framework of the EUMETSAT Satellite Application Facility on Ozone and Atmospheric Chemistry Monitoring (O3M-SAF).

GDP 4.8 HCHO column data are compared to independently retrieved HCHO columns using the scientific prototype algorithm developed and maintained at the Belgian Institute for Space Aeronomy (BIRA-IASB, Brussels, Belgium), using common GOME-2 level 1 data. GOME-2 HCHO column data are also compared to ground-based columns retrieved from MAX-DOAS measurements at the pilot station of Xianghe in the Beijing area (P.R. China).

A.2. Preliminary remarks

Validation techniques for HCHO column data derived from satellite measurements are in continuous development. This document details the progress of HCHO validation set-up for GOME-2 on MetOp-A and B, which at this stage concentrates on verification activities using the BIRA-IASB prototype and a limited number of MAX-DOAS observations performed by BIRA-IASB.

A.3. Plan of this document

After presentation of the GOME-2 Data Disclaimer for HCHO column products, this document is divided into the following sections:

A. Introduction
B. Validation Protocol
C. Step by step verification: GDP 4.7 against GDP 4.8 GOME-2 HCHO retrievals.
D. Step by step verification: GOME-2B against GOME-2A HCHO operational against scientific retrievals.
E. Step by step verification: Time-series above emission regions.
F. Comparison with ground-based HCHO observations.
G. Conclusions
H. References

B. VALIDATION PROTOCOL

B.1. Rationale and method

- We follow a validation protocol established within the O3M-SAF for trace gas data products. This consists in a step-by-step approach to validation where each sub-product is verified, i.e. for HCHO:
    - slant columns (SCD)
    - normalized slant columns (ΔSCD) (see [ATBD] and De Smedt et al., 2008 for more details about the reference sector correction)
    - air mass factors without cloud correction (AMF_{clear})
    - air mass factors with independent pixel cloud correction (AMF)
    - total vertical columns (VCD) (the bulk of the formaldehyde column lies in the lower troposphere, the contribution from the stratosphere is negligible).

- We also follow the overarching principles of the Quality Assurance Framework for Earth Observation [QA4EO], which establish the data quality strategy for the [GEOSS] and as such apply directly to [Copernicus], namely:
    - All data and derived products have associated with them a documented and fully traceable quality indicator (QI).
    - A quality indicator shall provide sufficient information to allow all users to readily evaluate the "fitness for purpose" of the data or derived product.
    - A quality indicator shall be based on a documented and quantifiable assessment of evidence demonstrating the level of traceability to internationally agreed (where possible SI) reference standards.

B.2. Reference data

The focus of this report is mainly the verification and validation of the improvements of the new GDP 4.8 version against GDP 4.7. The operational GDP 4.8 HCHO retrieval algorithm for METOP GOME-2 is fully described in the corresponding ATBD (DLR/GOME-2/ATBD/01). The scientific product used as reference has been described in several publications (De Smedt et al., 2008; 2010; 2012 and 2015). Here, the latest version (v14) of the BIRA-IASB GOME-2 HCHO retrieval is used (for more details, see De Smedt et al., 2015). The main specificities of this scientific product can be listed as follows:

- **Sc.v14**:
    - 3 inter-linked fitting intervals (339-364 nm for O_4, 328.5-359 nm for BrO, 328.5-346 nm for HCHO).
    - Fit of the GOME-2 slit function during the spectral calibration, using an asymmetric Gaussian line shape.
    - Radiance spectra selected daily in the remote Equatorial Pacific region are used as reference spectra in the DOAS equation.
    - Use of two additional cross-sections to better take into account O_3 absorption non-linearity with wavelength (Pukite et al., 2010).
    - Spike removal algorithm (Richter et al., 2011).

Following the previous verification reports, two inter-linked fitting intervals (332-359 nm for BrO, 328.5-346 nm for HCHO) have been implemented in GDP 4.8.

Table 1 summarizes the main characteristics and changes that have been implemented in GDP 4.8 compared to GDP 4.7. Tables 2 and 3 summarize the main characteristics of the scientific retrievals (v14) and the differences with the GDP 4.8 processor.

Table 1: Summary of DOAS settings for GOME-2A and B in the GDP 4.8 and the previous version 4.7

	GDP 4.7	GDP 4.8
Calibration	SAO96	SAO2010 (Chance&Kurucz, 2010)
Slit function	FM203(GOME-2A)/FM202(GOME-2B) from GOME-2 calibration key data (EUMETSAT, 2009)	FM203(GOME-2A)/FM202(GOME-2B) from GOME-2 calibration key data (EUMETSAT, 2009)
Polynomial	5^{th} order	5^{th} order
Intensity offset	linearized (inversed solar)	linearized (inversed earth-shine)
H_2CO	Meller&Moortgat, 2000	Meller&Moortgat, 2000
O_3	Brion et al., 1998/Malicat et al. 1995	Brion et al., 1998/Malicat et al. 1995
BrO	Fleischmann et al., 2004	Fleischmann et al., 2004
NO_2	Vandaele et al., 2002	Vandaele et al., 2002
OClO	Bogumil et al., 2003	Bogumil et al., 2003
Ring effect	2 ring cross sections calculated using SCIATRAN (Rozanov et al., 2001)	2 ring cross sections calculated using SCIATRAN (Rozanov et al., 2001)
Polarisation vectors	Eta/Zeta from GOME-2 calibration key data (EUMETSAT, 2009)	Eta/Zeta GOME-2 calibration key data (EUMETSAT, 2009)
Non-linear O_3 absorption effects	-	2 pseudo cross sections from Taylor expansion of wavelength and optical depth (Puķīte et al., 2010)
Fitting interval 1	-	332-359 nm
Included cross sections	-	H_2CO(298K), NO_2(220K), OClO(293K), O_3(228K/243K), 2 pseudo cross sections (O_3O_3/λO_3), Zeta/Eta, Ring1/Ring2, BrO(223K)
Fitting interval 2	328.5-346 nm	328.5-346 nm
Included cross sections	H_2CO(298K), NO_2(220K), OClO(293K), O_3(228K/243K), Zeta/Eta, Ring1/Ring2, BrO(223K)	H_2CO(298K), NO_2(220K), OClO(293K), O_3(228K/243K), 2 pseudo cross sections (O_3O_3/λO_3), Zeta/Eta, Ring1/Ring2 *BrO (from fitting interval 1)*

Table 2 : DOAS settings used to retrieve HCHO slant columns from GOME-2 spectra in scientific retrievals based on version Sc.v14.

Calibration	Accurate solar atlas (Chance and Kurucz, 2010)
Slit function	Asymmetric Gaussian slit function fitted during calibration (De Smedt et al., 2012)
Reference spectrum	Daily average of radiance spectra selected in the remote equatorial Pacific
Polynomial	5th order
Intensity offset	Linear offset (inversed earth-shine)
Hot pixels treatment	Iterative spike removal algorithm (Richter et al., 2011)
Absorption cross-section datasets	
H_2CO	Meller and Moortgat (2000)
O_3	Brion et al. (1998); Daumont et al. (1992); Malicet et al. (1995)
BrO	Fleischmann et al. (2004)
NO_2	Vandaele et al. (2002)
O_2-O_2 (O_4)	Thalman and Volkamer (2013)
Ring effect	2 Ring cross-sections calculated in an ozone containing atmosphere for low and high SZA, using LIDORT RRS (Spurr et al., 2008).
Polarisation vectors	Eta and Zeta from the GOME-2 calibration key data (EUMETSAT, 2009)
Non-linear O_3 absorption effect	2 pseudo-cross sections from the Taylor expansion of the wavelength and the O_3 optical depth (Puķīte et al., 2010).
Fitting interval 1: O_4	**339-364 nm**
Included cross-sections	O_4 (293K), O_3 (228K), BrO (223K), H_2CO (298K), NO_2 (220K), Ring1, Ring2, eta, zeta
Fitting interval 2: BrO	**328.5-359 nm**
Included cross-sections	BrO (223K), H_2CO (298K), O_3 (228K and 243K), NO_2 (220K), O_4 (293K, not fitted), Ring1, Ring2, O_3L, O_3O_3, eta, zeta
Fitting interval 3: H_2CO	**328.5-346 nm**
Included cross-sections	H_2CO (298K), O_3 (228K and 243K), BrO (223K, not fitted), NO_2 (220K), O_4 (293K, not fitted), Ring1, Ring2, O_3L, O_3O_3

Table 3: Comparison of the a priori data used in the GDP 4.8 processor and in the scientific retrievals for the air mass factor calculations.

Quantity	GDP 4.8	Scientific retrievals
Surface Reflectance	TOMS/GOME climatology	Kleipool database derived from OMI data, 2008
Atmospheric profiles	Climatology based on IMAGESv2 profiles	Daily IMAGESv2 profiles
Clouds	OCRA/ROCINN v3.0	FRESCOv6
Surface elevation	GTOP30	ETOPO5 at 0.5° horizontal resolution (www.ngdc.noaa.gov)

C. VERIFICATION OF INDIVIDUAL COMPONENTS OF THE GOME-2 PROCESSING CHAIN: GDP 4.8 AGAINST GDP 4.7.

C.1. Verification of Slant Column Density

To verify the improvements of GDP v4.8 against v4.7, the results of the two processor versions are compared along a single orbit of GOME-2A in 2007 (Figure 1), GOME-2A in 2013 (Figure 2), and GOME-2B in 2013 (Figure 3). Three parameters of the fit results are compared: the HCHO slant columns (SCD), the HCHO slant columns normalized in the remote Pacific Ocean (dSCD), and the DOAS fit residuals (RMS).

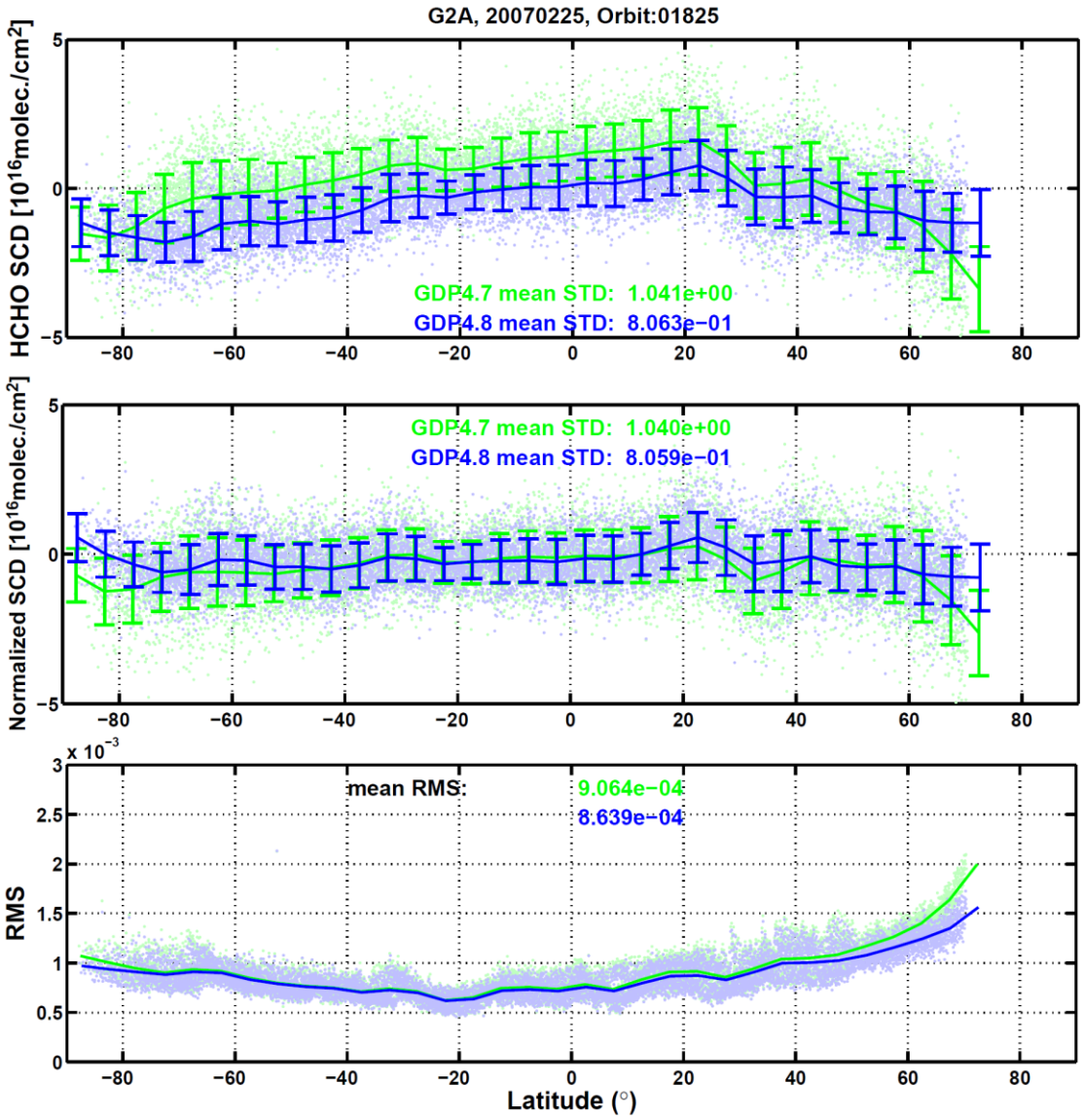

Figure 1: GDP 4.7 (in green) versus GDP 4.8 (in blue) HCHO retrievals for one orbit of GOME-2 on METOP-A (25/02/2007, orbit nr. 1835). Dots are individual measurements; lines are averages within 5° latitude-bands. First panel: raw slant columns (SCD), second panel: normalized slant columns (dSCD), third panel: residuals of the fit (RMS). Mean standard deviation of the slant columns and RMS are given inset.

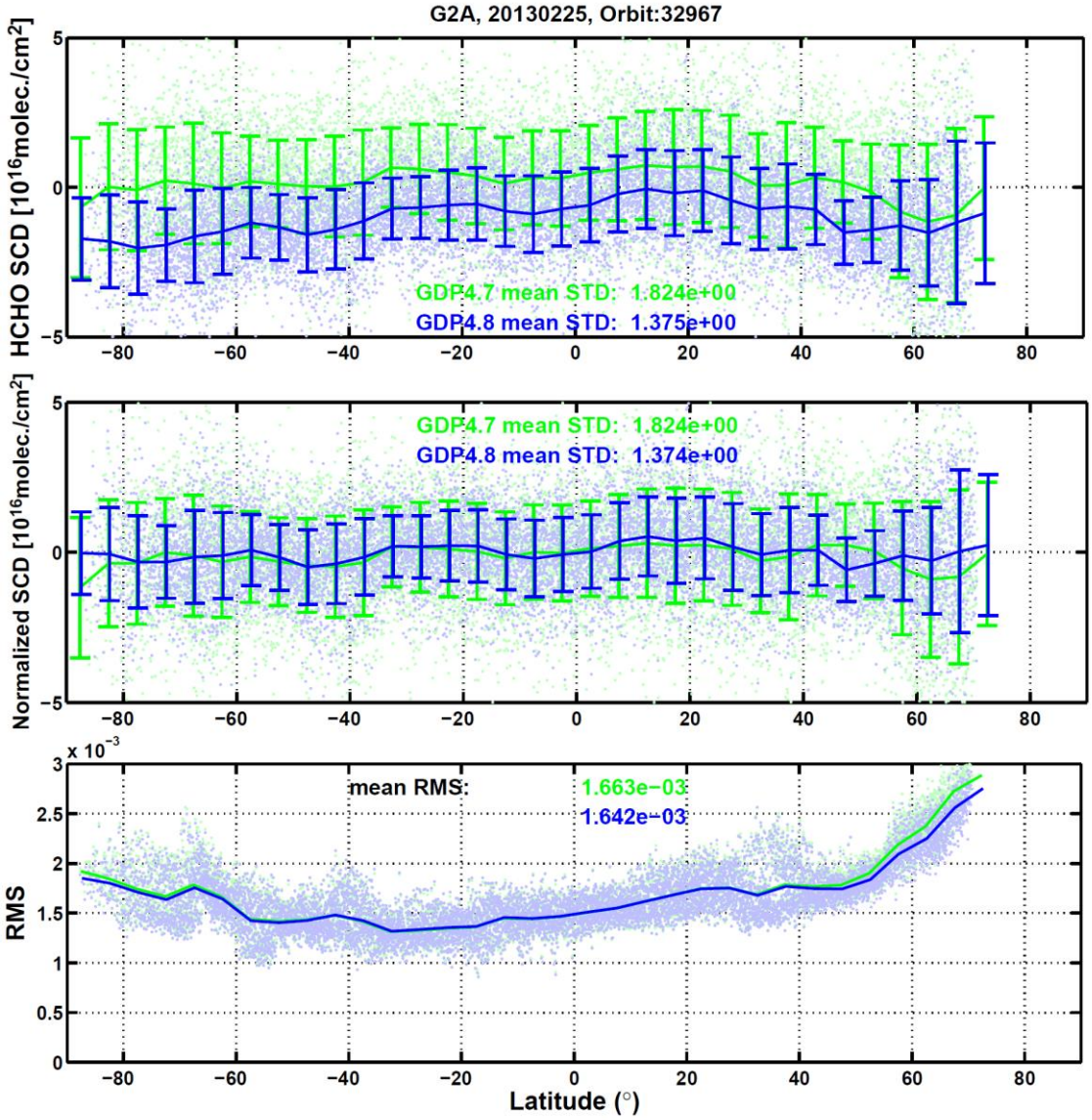

Figure 2: GDP 4.7 (in green) versus GDP 4.8 (in blue) HCHO retrievals for one orbit of GOME-2 on METOP-A (25/02/2013, orbit nr. 32967). Dots are individual measurements; lines are averages within 5° latitude-bands. First panel: raw slant columns (SCD), second panel: normalized slant columns (dSCD), third panel: residuals of the fit (RMS). Mean standard deviation of the slant columns and RMS are given inset.

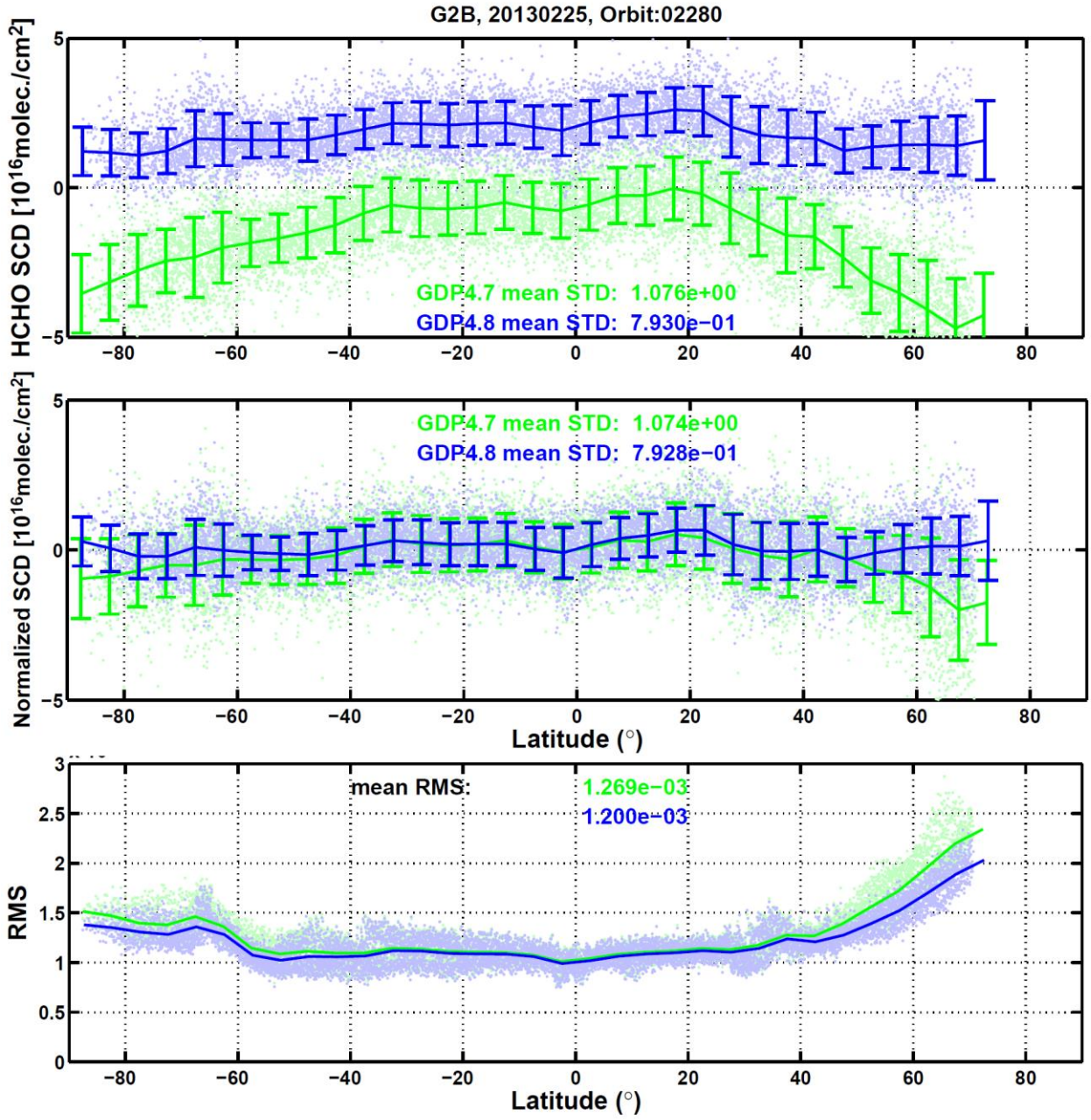

Figure 3: GDP 4.7 (in green) versus GDP 4.8 (in blue) HCHO retrievals for one orbit of GOME-2 on METOP-B (25/02/2013, orbit nr. 2290). Dots are individual measurements; lines are averages within 5° latitude-bands. First panel: raw slant columns (SCD), second panel: normalized slant columns (dSCD), third panel: residuals of the fit (RMS). Mean standard deviation of the slant columns and RMS are given inset.

From inspection of Figures 1, 2, and 3 we conclude the following:

- The current quality of the MetOp GOME-2 radiance and irradiance spectra in the 328.5-346 nm and 332-359 nm spectral intervals enables stable DOAS retrievals.
- Compared to the previous GDP 4.7 version, the GDP 4.8 HCHO slant columns present a level of noise reduced by -17% in 2007 and -25% in 2013 for GOME-2A and by -26% in 2013 for GOME-2B. This improvement is brought by the use of the two inter-linked fitting windows, including the pre-fit of BrO. The noise reduction level is in line with the numbers obtained in the scientific product (De Smedt et al., 2012 and the previous O3SAF verification report).

- The underestimation of HCHO SCD, and RMS at large SZA (higher O_3 SCD) are reduced by the introduction of two pseudo-cross sections from the Taylor expansion of the wavelength and the O_3 optical depth. This is also in line with what is expected from the scientific product results.
- Before normalisation of the SCD in the remote Pacific, the improvement of GDP 4.8 over GDP 4.7 is more pronounced in the case of GOME-2B than GOME-2A. Although the reason of the large negative offset of HCHO SCD (when only 1 fitting window is used, 328.5-346) in GOME-2B is not completely understood, this result is also found in the scientific product.
- After application of the reference sector correction, the HCHO slant columns are correctly brought back around zero at all latitudes.
- The degradation of the GOME-2/METOP-A instrument between 2007 and 2013 resulted in an increase of the noise and of the RMS by almost a factor of 2.
- GOME-2B HCHO corrected slant columns, fit residuals, and scatters are comparable to those obtained from GOME-2A spectra in 2007.

C.2 Verification of Vertical Column Density

To verify the improvements of GDP v4.8 against v4.7, the results of the two processor versions are compared along a single orbit of GOME-2A in 2007. For the verification of the HCHO VCD, two sets of parameters are compared: the cloud free VCD and AMF (VCD free, AMF free), and the cloud-corrected VCD and AMF (VCD total, AMF total). Figures 4 to 6 illustrate the status of the comparisons between GDP4.7 and GDP4.8 applied to GOME-2A in 2007. The same conclusions can be drawn from inspections of GOME-2A and GOME-2B in 2013.

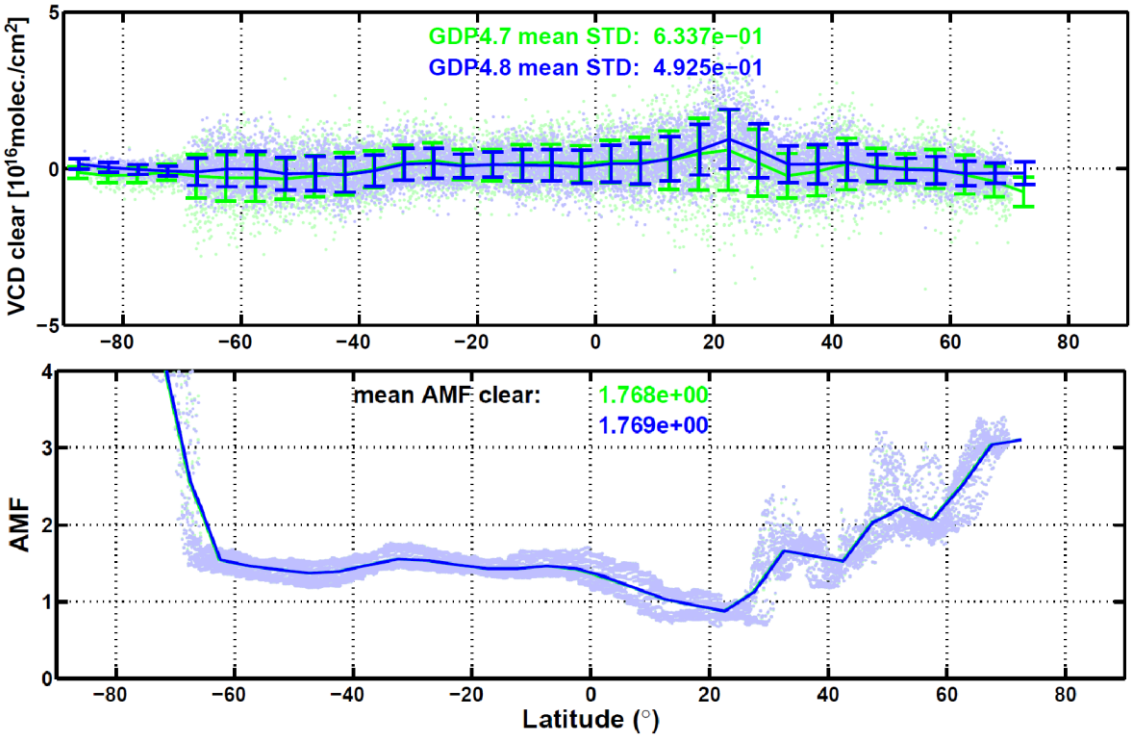

Figure 4: GDP 4.7 (in green) versus GDP 4.8 (in blue) HCHO vertical columns, without cloud correction, for one orbit of GOME-2 on METOP-A (25/02/2007, orbit nr. 1835). Dots are individual measurements; lines are averages within 5° latitude-bands. First panel: clear-sky vertical columns (VCD_{clear}), second panel: clear-sky AMFs (AMF_{clear}).

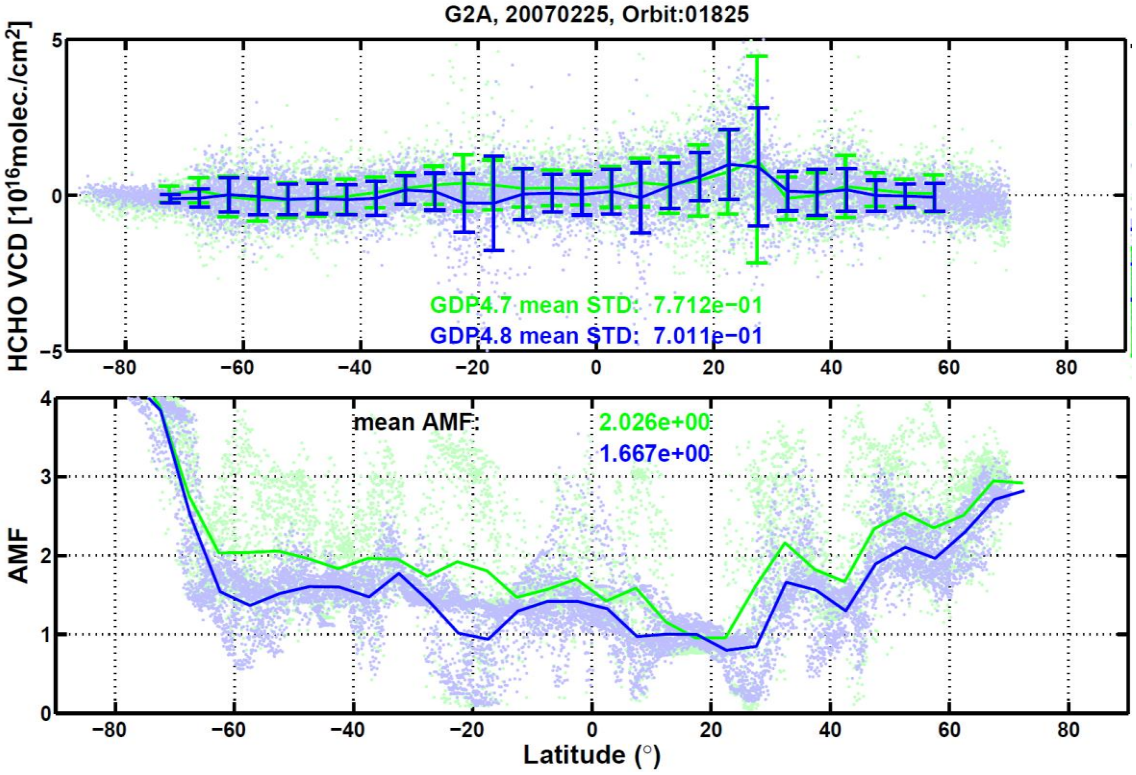

Figure 5: GDP 4.7 (in green) versus GDP 4.8 (in blue) HCHO vertical columns, with cloud correction, for one orbit of GOME-2 on METOP-A (25/02/2007, orbit nr. 1835). Dots are individual measurements; lines are averages within 5° latitude-bands. First panel: vertical columns (VCD), second panel: AMFs (AMF).

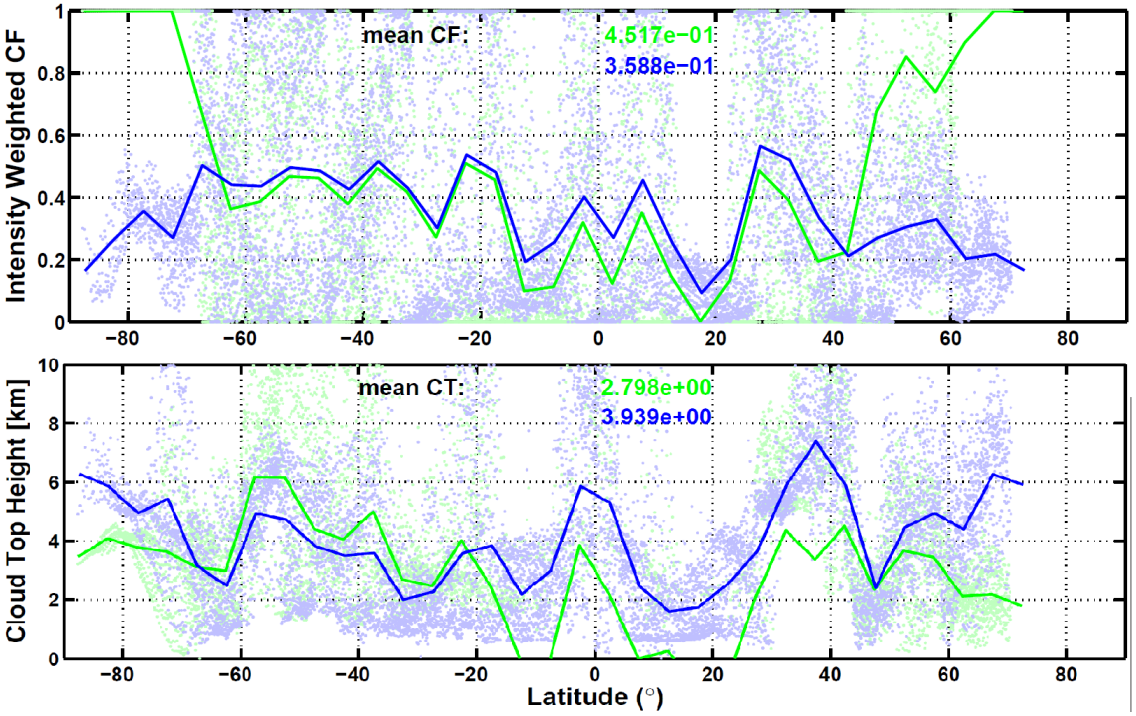

Figure 6: GDP 4.7 (in green) versus GDP 4.8 (in blue) cloud parameters for one orbit of GOME-2 on GOME-2 on METOP-A (25/02/2007, orbit nr. 1835). First panel: intensity weighted cloud fraction (OCRA), second panel: cloud top altitude (ROCINN).

From inspection of Figure 4, Figure 5, and Figure 6 we conclude the following:

- Cloud free AMFs are identical between GDP4.7 and GDP 4.8. This is as expected since the albedo, a-priori profiles, and elevation maps have not been updated.
- The standard deviation of the HCHO VCD, not corrected for clouds, is 20% lower in GDP 4.8 than in GDP 4.7 (in 2007), thanks to the improvement of the slant columns.
- The cloud product has been updated between the two versions of the processor (Lutz et al., 2015). The net result on the cloud corrected HCHO AMF is a decrease of the total AMF by about 17%. This is mainly due to an increase of the mean cloud top height of about 1km in average, in agreement with the expected AMF dependency with CTH.
- The cloud correction tends to increase the HCHO vertical columns and their standard deviations. This effect is more marked with the GDP 4.8 cloud product than with GPD 4.7.
- It is beyond the scope of this report to validate the OCRA/ROCIN cloud product. However, the cloud effect is further discussed in the following section.

C.3 Effect of the new cloud product on the HCHO VCDs

The influence of cloud properties on the HCHO retrieval can be divided into two parts:

1. the effect of the cloud correction on the AMF calculation
2. the sampling effect of cloud free observation selection.

Both effects are investigated based on monthly averaged HCHO columns, from GOME-2A in February 2007 and 2013, and from GOME-2B in February 2013.

The first effect is evaluated by comparing the differences of the HCHO vertical columns using the either a tropospheric AMF ($AMF_{trop}=AMF_{clear}*(1-CRF)+AMF_{cloud}*CRF$) or AMF_{clear} (without cloud correction). Comparisons are shown in Figure 7. As the clear-sky AMFs have not changed between GDP 4.7 and GDP 4.8, the differences seen are related to the cloud correction itself, and therefore to the cloud properties.

GDP4.7	GDP4.8
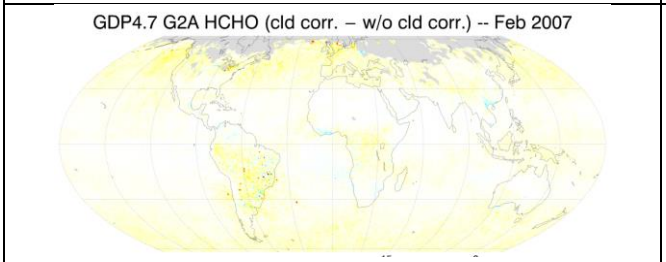	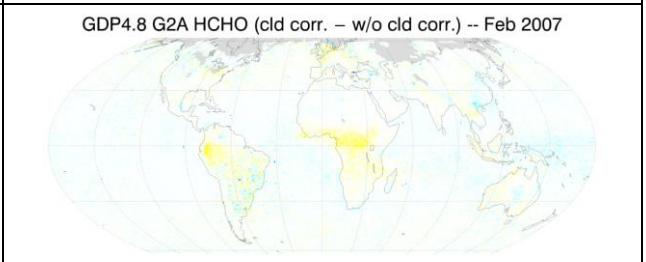
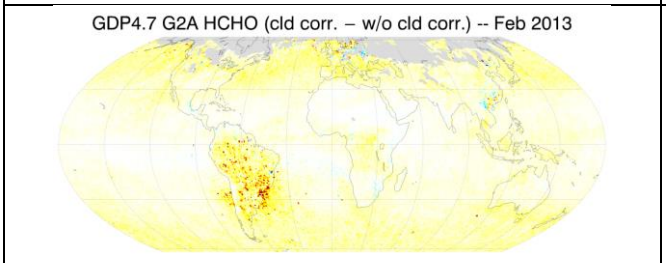	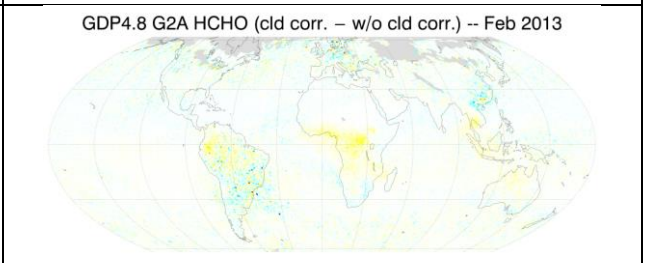
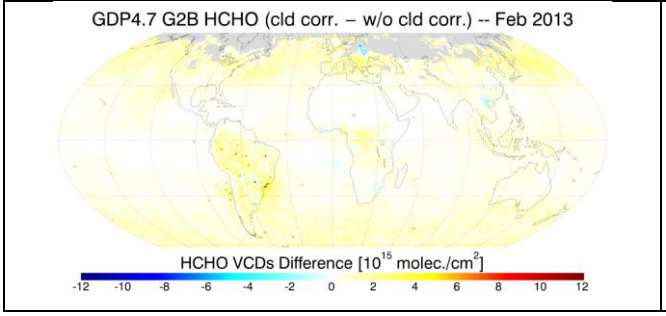	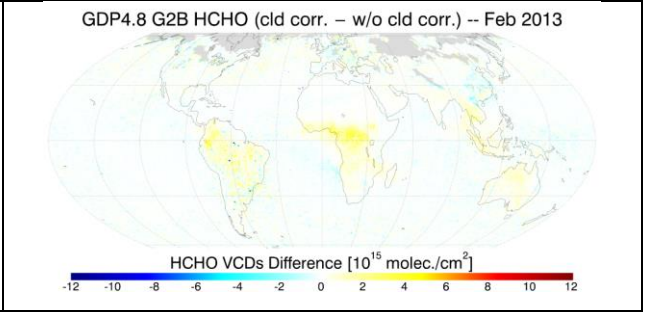

Figure 7: Illustration of the cloud correction effect. Differences between the HCHO VCD obtained using the cloud-corrected AMF_{trop} and using the clear-sky AMF_{clear} (without cloud correction). Results are shown for GDP 4.7 (left panels) and GDP 4.8 (right panels), for GOME-2A in Feb. 2007 (upper panels) and Feb. 2013 (center panels), and GOME-2B in Feb. 2013 (lower panels).

The second effect of sampling due to the selection of low cloud observations is estimated based on the GDP 4.8 HCHO VCDs obtained using clear-sky AMFs, and the two versions of the cloud radiance fractions from GDP 4.7 and GDP 4.8. In Figure 8, are shown the differences of monthly HCHO columns obtained using a cloud radiance selection threshold of 50%, respectively based on GDP 4.7 or GDP 4.8 cloud product.

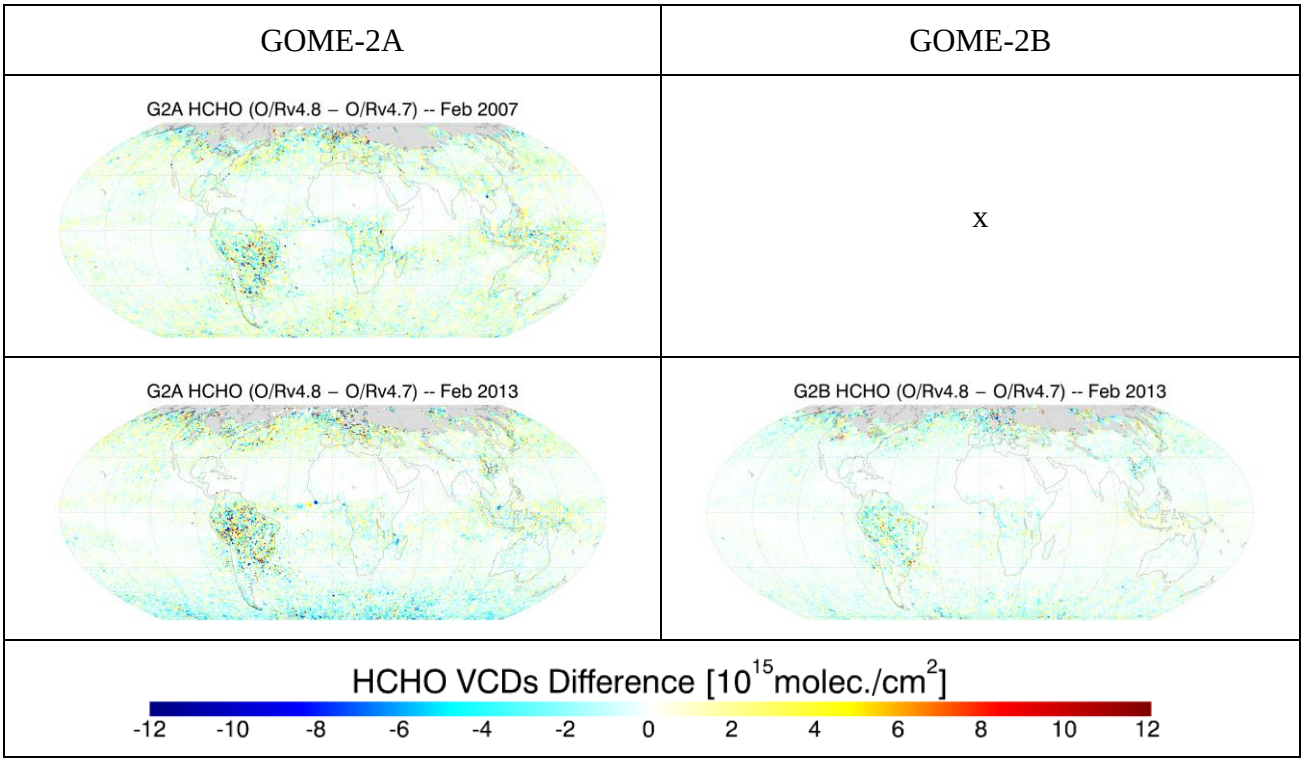

Figure 8: Cloud sampling effect resulting from the new cloud product. Differences of monthly averaged HCHO VCD (GDP4.8) using a cloud filtering based either on CRF(GDP 4.7) or CRF(GDP 4.8). The CRF threshold is fixed to 50%.

From inspection of Figure 7 and Figure 8, we conclude the following:

1. Effect of cloud correction on HCHO retrieval

- Difference between GDP 4.7 and 4.8
  - GDP 4.7: Non-physical positive effects of the cloud correction on the HCHO VCDs are observed at high latitudes.
  - GDP 4.8: The cloud correction has a marked effect mainly over tropical regions (positive effect over land, and slightly negative effect over ocean).
- Difference between GOME-2A in 2007 and in 2013
  - GDP 4.7: The effect of cloud correction is systematically larger in 2013 than in 2007.
  - GDP 4.8: The cloud correction effect is constant. Only some slight differences over the polluted regions in south hemisphere are observed (East US, Europe and East China).
- Difference between GOME-2A and GOME-2B
  - GDP4.7: The cloud algorithm is strongly affected by the instrumental degradation of GOME-2A, the cloud correction impact is therefore more consistent between GOME-2A in 2007 and GOME-2B in 2013.

2. GDP 4.8: The degradation impact on the clouds has been improved, and consistent cloud correction effects are observed between GOME-2A and GOME-2B also in 2013. Sampling effect due to the selection of low cloud observations
   - In general, the sampling effect is very similar between the two cloud product (4.7 and 4.8). Both versions discriminate similarly the "cloud-free" from the cloudy pixels.
   - Some differences are observed over Tropical regions and at high latitudes, because the statistics are less favorable due to the lack of sampling. Indeed, those regions are always covered by clouds, and only a few 'cloud-free' satellite measurements are taken into account in the monthly averages.
   - A systematic negative bias is found over high latitudes for GOME-2A 2013, this is probably due to GOME-2A instrumental degradation effects on the cloud retrievals in GDP 4.7.

D. VERIFICATION OF INDIVIDUAL COMPONENTS OF THE GOME-2 PROCESSING CHAIN: GOME2-A AGAINST GOME2-B IN THE OPERATIONAL AND IN THE SCIENTIFIC PRODUCTS

To verify the consistency between GOME-2A and GOME-2B results, the retrievals of the two instruments are compared along a single orbit of GOME-2A and GOME-2B in 2013, separately for the GDP4.8 processor and for the scientific prototype Sc.v14 (Figure 9 and Figure 10). Four parameters of the fit results are compared: the HCHO slant columns (SCD), the HCHO slant columns normalized in the remote Pacific Ocean (dSCD), the DOAS fit residuals (RMS), and the HCHO vertical columns (VCD).

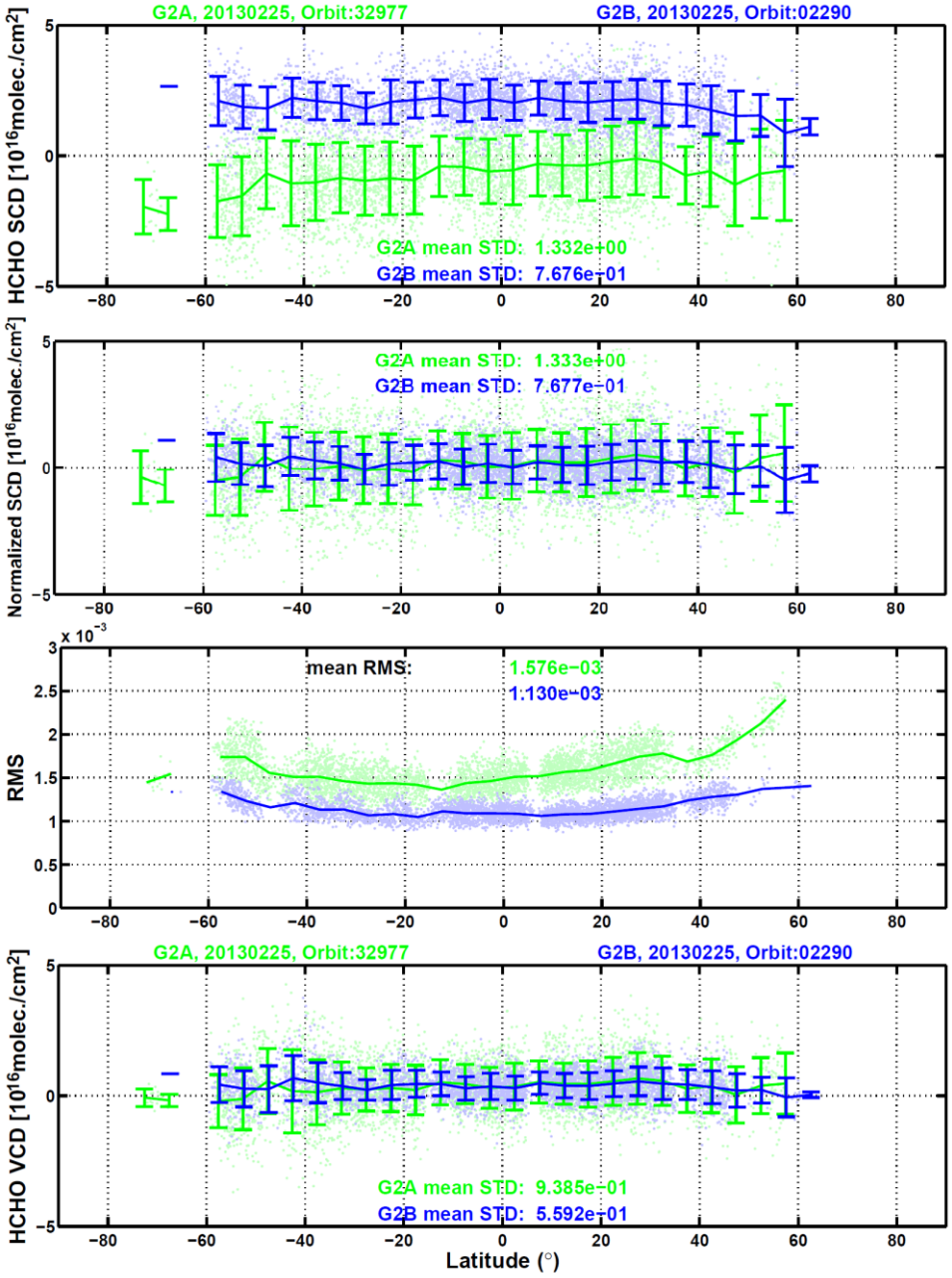

Figure 9: GDP 4.8 HCHO retrievals for one orbit of GOME-2 on METOP-A (green, 25/02/2013, orbit nr. 32977) and METOP-B (bleu, 25/02/2013, orbit nr. 2290), both in 2013. Dots are individual measurements; lines are averages within 5° latitude-bands. First panel: slant columns (SCD), second panel: normalized slant columns (dSCD), third panel: residuals of the fit (RMS), fourth panel: HCHO vertical columns (VCD). Standard deviations of the HCHO columns and mean RMS are given inset.

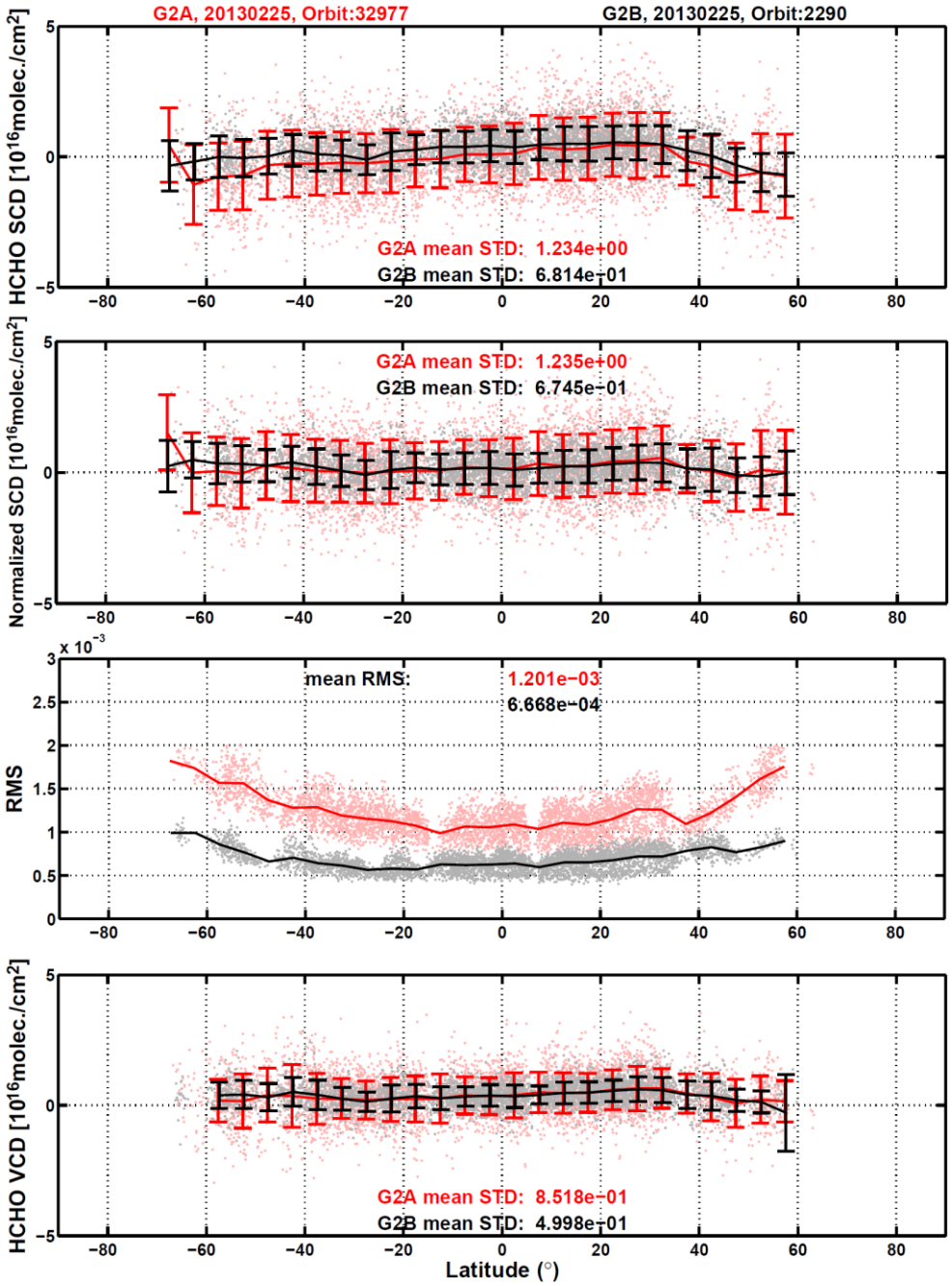

Figure 10: Sc.v14 HCHO retrievals for one orbit of GOME-2 on METOP-A (green, 25/02/2013, orbit nr. 32977) and METOP-B (bleu, 25/02/2013, orbit nr. 2290), both in 2013. Dots are individual measurements; lines are averages within 5° latitude-bands. First panel: slant columns (SCD), second panel: normalized slant columns (dSCD), third panel: residuals of the fit (RMS), fourth panel: HCHO vertical columns (VCD). Standard deviations of the HCHO columns and mean RMS are given inset.

From inspection of Figure 9 and Figure 10, we conclude the following:

- The degradation of GOME-2A spectra along the years tends to increase the negative offsets of HCHO (uncorrected) slant columns, both in the UPAS and the scientific products. However, the use of remote radiance spectra as background for the DOAS analysis in the scientific algorithm allows for a reduction of the offsets.
- Ultimately, the negative offsets in slant columns are efficiently corrected by the reference sector correction, both in the UPAS and the scientific products.

- After the reference sector correction, normalized HCHO slant columns are very consistent between GOME-2A and GOME-2B, both in the operational and in the scientific products.
- The same is true concerning the vertical columns.
- Although the comparison of GOME-2A and GOME-2B in 2013 shows a good level of consistency, the noise level of GOME-2A is larger by approximately a factor 2, due to degradation effects. This effect is mitigated in the scientific algorithm by the use of radiance spectra as reference and a dynamically adjusted slit function, nevertheless the impact of the degradation is clearly apparent in both products.

Results confirm that HCHO VCDs derived from GOME-2B are of equivalent quality and fully consistent with those derived from GOME-2A. Similar conclusions can be reached using both GDP4.8 and scientific retrievals. To verify the consistency between GOME-2A and GOME-2B results, and the improvements of GDP v4.8 against v4.7, maps of monthly (Figure 11) and yearly averaged (Figure 12) HCHO vertical columns are displayed for GOME-2A in 2007 and GOME-2B in 2013, for the two versions of GDP and for the prototype Scv14 algorithm. Results are shown at the beginning of each sensor lifetime in order to illustrate the improvement of the algorithm performances, without any degradation effect.

VCD	GOME-2 METOP-A	GOME-2 METOP-B
GDP 4.7	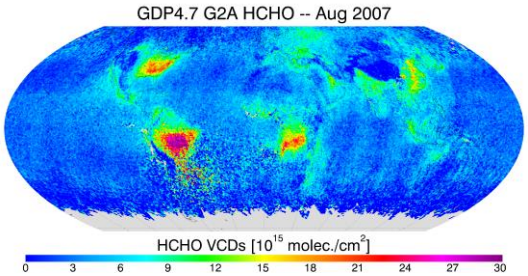	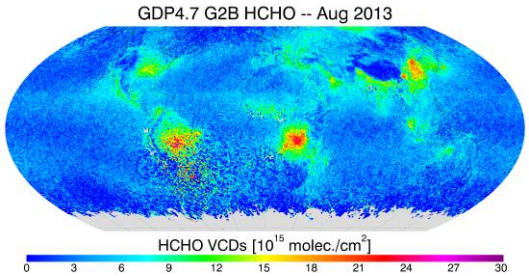
GDP 4.8	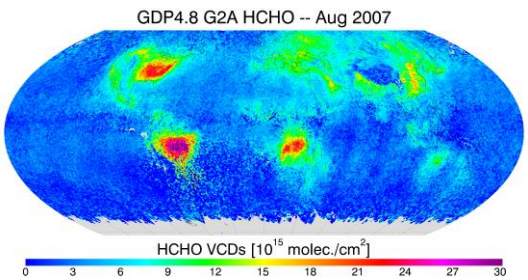	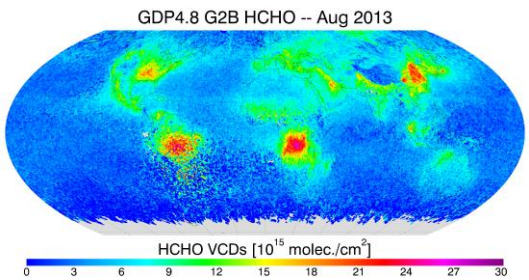
Sc.v14	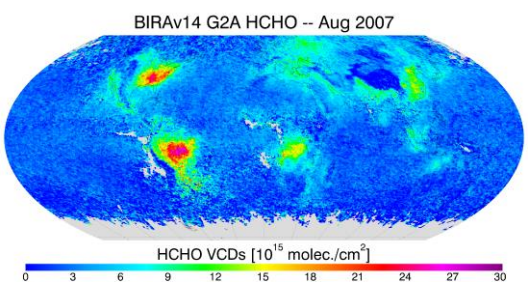	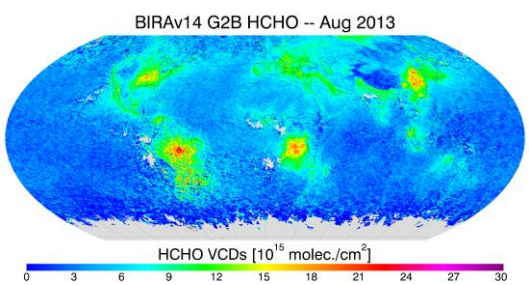

Figure 11: GOME-2 HCHO monthly averaged vertical columns for August 2007 and 2013 (CRF<50%).

VCD	GOME-2 METOP-A 2007	GOME-2 METOP-B 2013
GDP 4.7	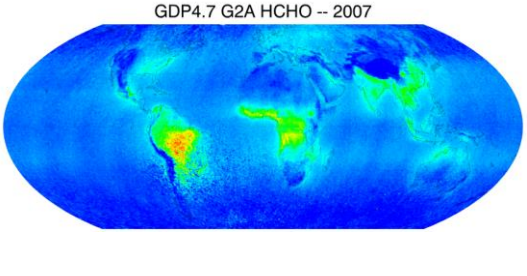	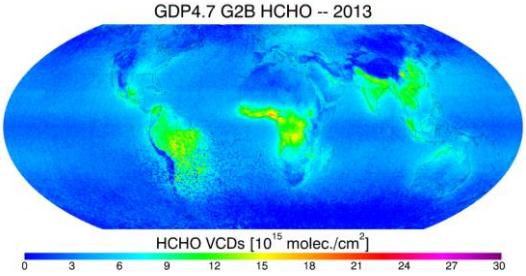
GDP 4.8	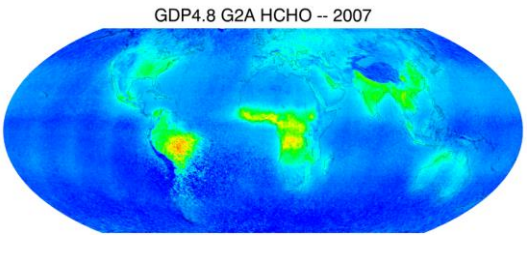	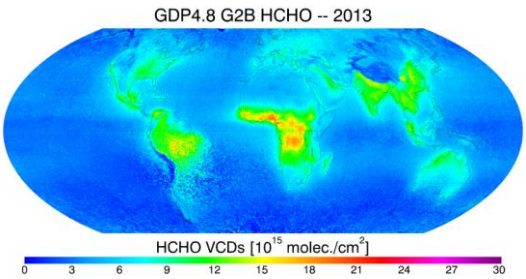
Sc. v14	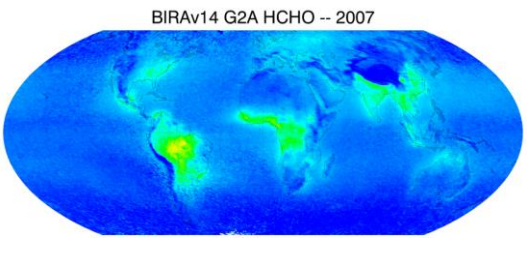	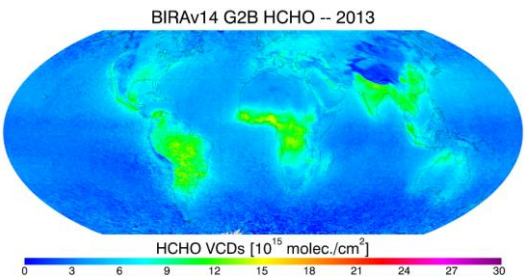

Figure 12: GOME-2 HCHO yearly averaged vertical columns for 2007 and 2013 (CRF<50%).

- The overall improvement of GDP 4.8 over GDP 4.7 data products is clearly apparent, with a noticeable decrease of the noise on the observations and less negative artefacts at high latitudes and over mountains, both for GOME-2A and GOME-2B.
- Despite an overall good consistency between GOME-2A and GOME-2B results, we observe slightly larger background columns retrieved from GOME-2B compared to GOME-2A, both in the operational and in the scientific products.
- Despite an overall good consistency between operational and scientific products, we observe differences between the HCHO vertical columns that are mainly due to different input parameters in the AMF calculations (surface albedo, cloud product, a priori profiles), but also to differences in the spectral fit settings (inclusion of O_4 cross-section in the large interval).
- While O4 absorption can be fitted by the polynomial in the small interval (328.5-346), it is not the case anymore in the large interval (328.5-359). It is our recommendation to include this cross-section in both intervals.
- The South-Atlantic anomaly (SAA) impact is less pronounced in the scientific product owing to the iterative spike removal algorithm that has been implemented.
- Regional comparisons based on monthly averaged columns are shown in the next section.

We acknowledge also the inclusion of total column averaging kernels, provided together with the integrated HCHO vertical columns. An example of comparison between GDP 4.8 and Sc.v14 is given in Figure 13. Differences are due to the different AMFs, since the averaging kernel is defined as the scattering weighting function divided by the total AMFs.

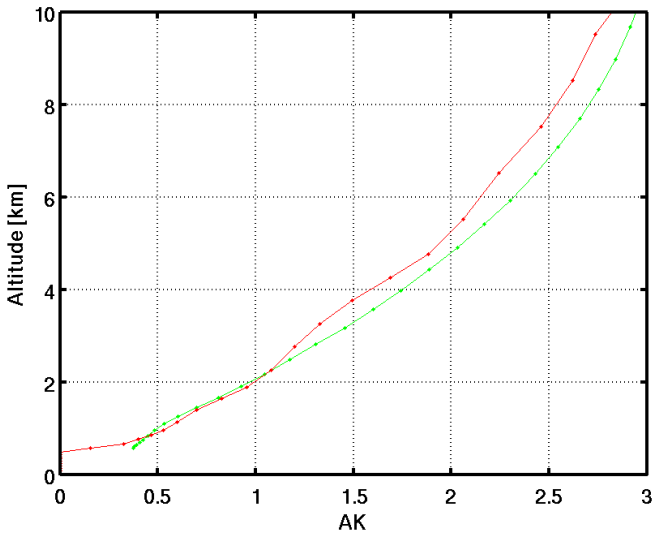

Figure 13: Example of Averaging Kernel in GDP 4.8 (green line) and Sc.v14 (red line) HCHO products for a single observation of GOME-2A on 25/02/2013, orbit 32967. Difference in surface albedo and cloud properties explain differences in AK.

E. VERIFICATION OF INDIVIDUAL COMPONENTS OF PROCESSING CHAINS: TIME-SERIES ABOVE EMISSION REGIONS

In this section, time-series of GOME-2A and GOME-2B HCHO data products are presented for a selection of emission regions (listed in Table 4), since 2007. Both operational (GDP 4.8) and scientific (v14) data are considered. Observations with cloud radiance fraction above 0.5 have been excluded from the monthly means. The individual components of the HCHO VCD processing chain are compared separately, in order to investigate possible compensating errors. In the following figures (Figure 14 to Figure 24), the different steps of the HCHO VCD retrieval are compared. This includes:

- The tropospheric vertical column (VCD).
- The normalized slant column (ΔSCD
- The DOAS fit RMS which is a good indicator of the fit quality.
- The standard deviations of the columns.
- The clear-sky air mass factor (AMF_{clear}) and the cloud-corrected (total tropospheric) air mass factor (AMF).

Table 4: List of the emissions regions considered for the GOME-2 comparisons.

Region	Lat Min	Lat Max	Long Min	Long Max
Northern Australia	-19	-10	123	145
Northern China	29	37	112	121
India	15	24	75	85
South Asia	12	22	98.5	110
Indonesia	-5	5	98	118
Northern Africa	3	14	-14	12
Equatorial Africa	-5	8	14	28
Southern Africa	-15	-5	10	30
Southeastern US	30	40	-95	-75
Guatemala	12.5	17.5	-95	-85
Mexico	15	20	-103	-88
Amazonia	-10	5	-75	-50

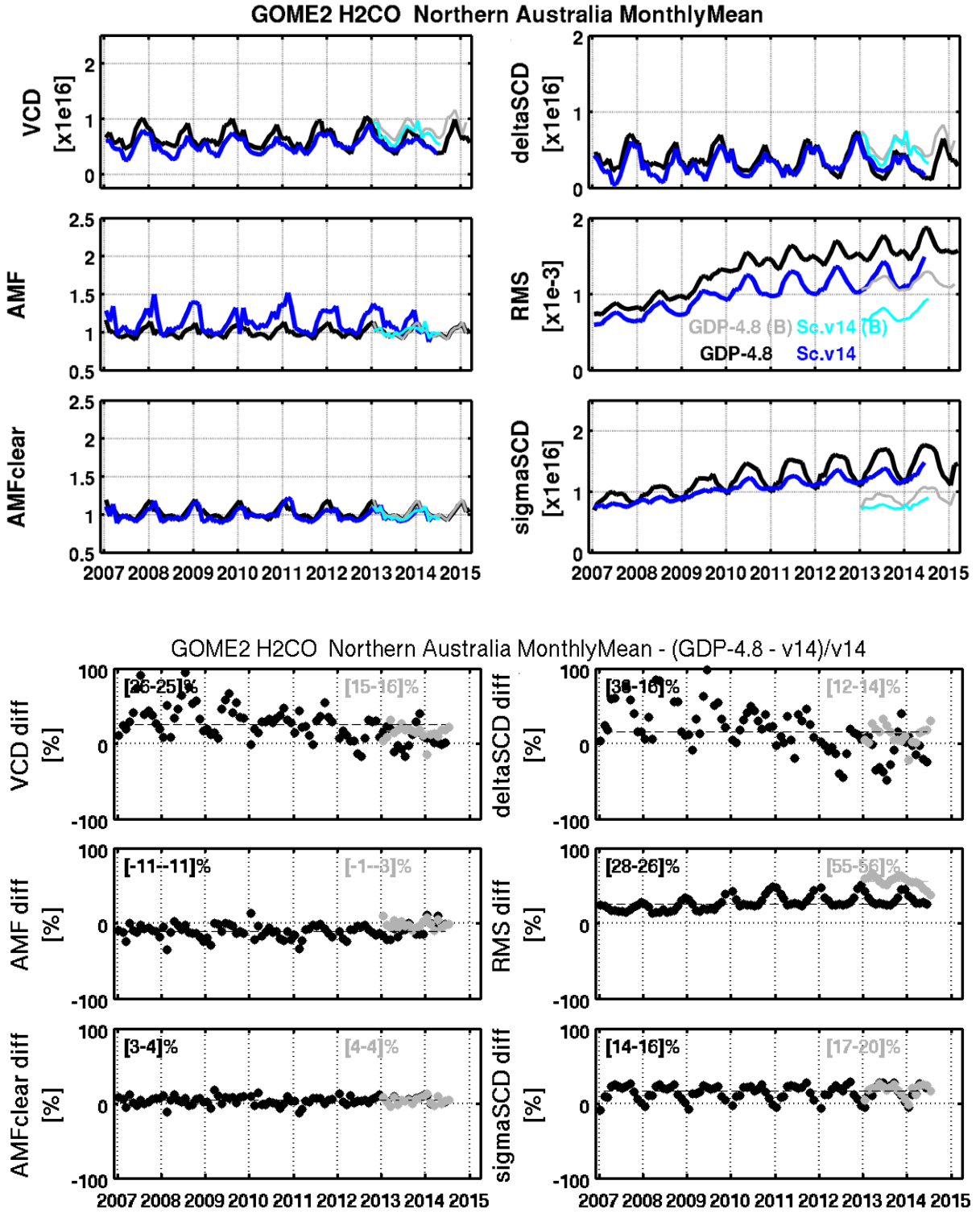

Figure 14: Upper panel: GDP-4.8 and Sc.v14 HCHO comparison from 2007 to mid-2014, for both GOME-2A (black and blue respectively) and METOP-B (cyan and grey respectively) in the Northern Australian region. The different panels present HCHO vertical columns (VCD), the normalized slant columns (deltaSCD), the standard deviation of the deltaSCD (sigmaSCD), the residuals of the fit (RMS), the total air mass factors (AMF) and the clear-sky air mass factors (AMF_{clear}). Lower panel: Relative differences between the GDP-4.8 and Sc.v14 products, respectively for GOME-2A (black) and for GOME-2B (grey). Numbers inset are the mean and median differences over the time series for each satellite instrument.

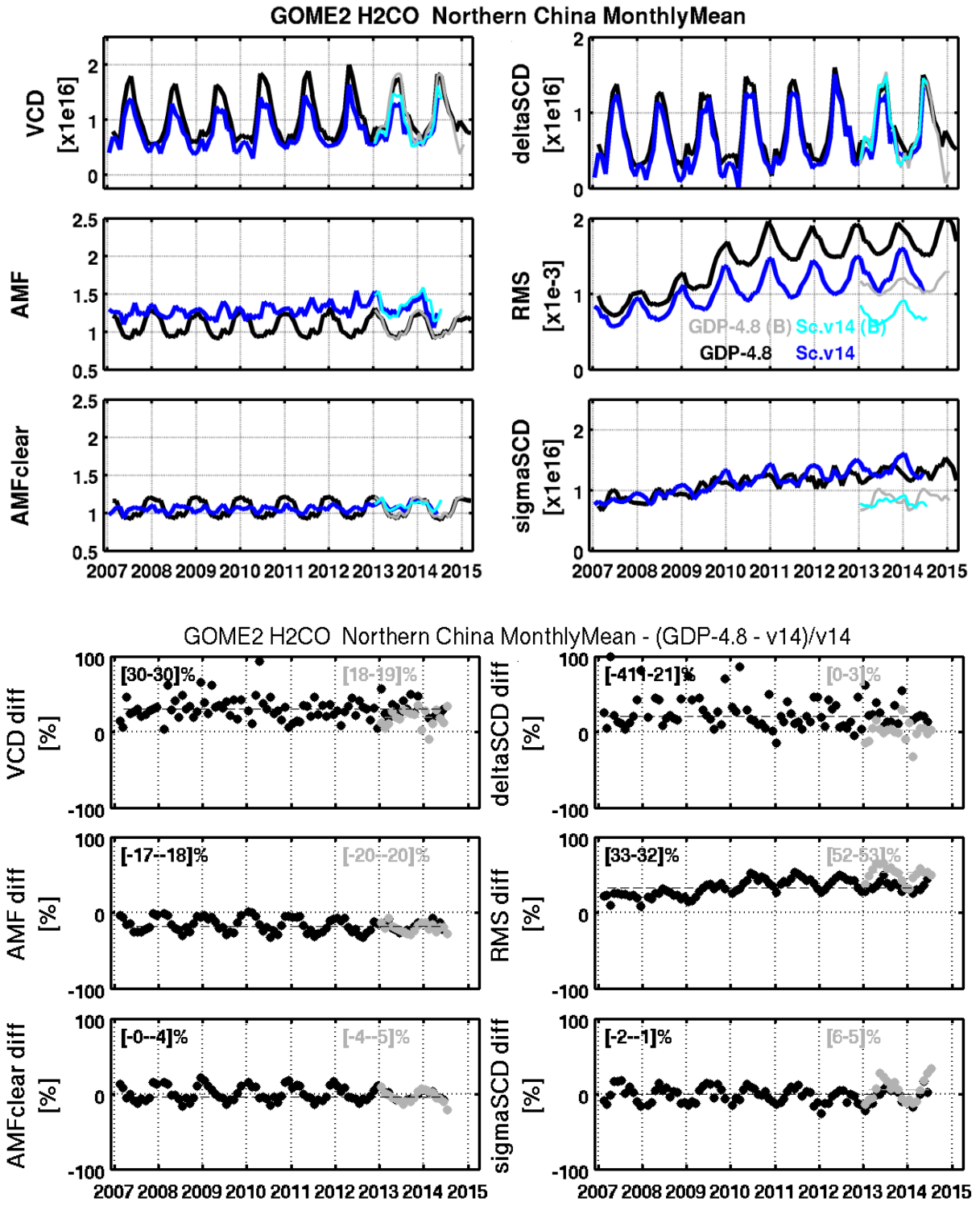

Figure 15: same as Figure 14, but for the Northern China region.

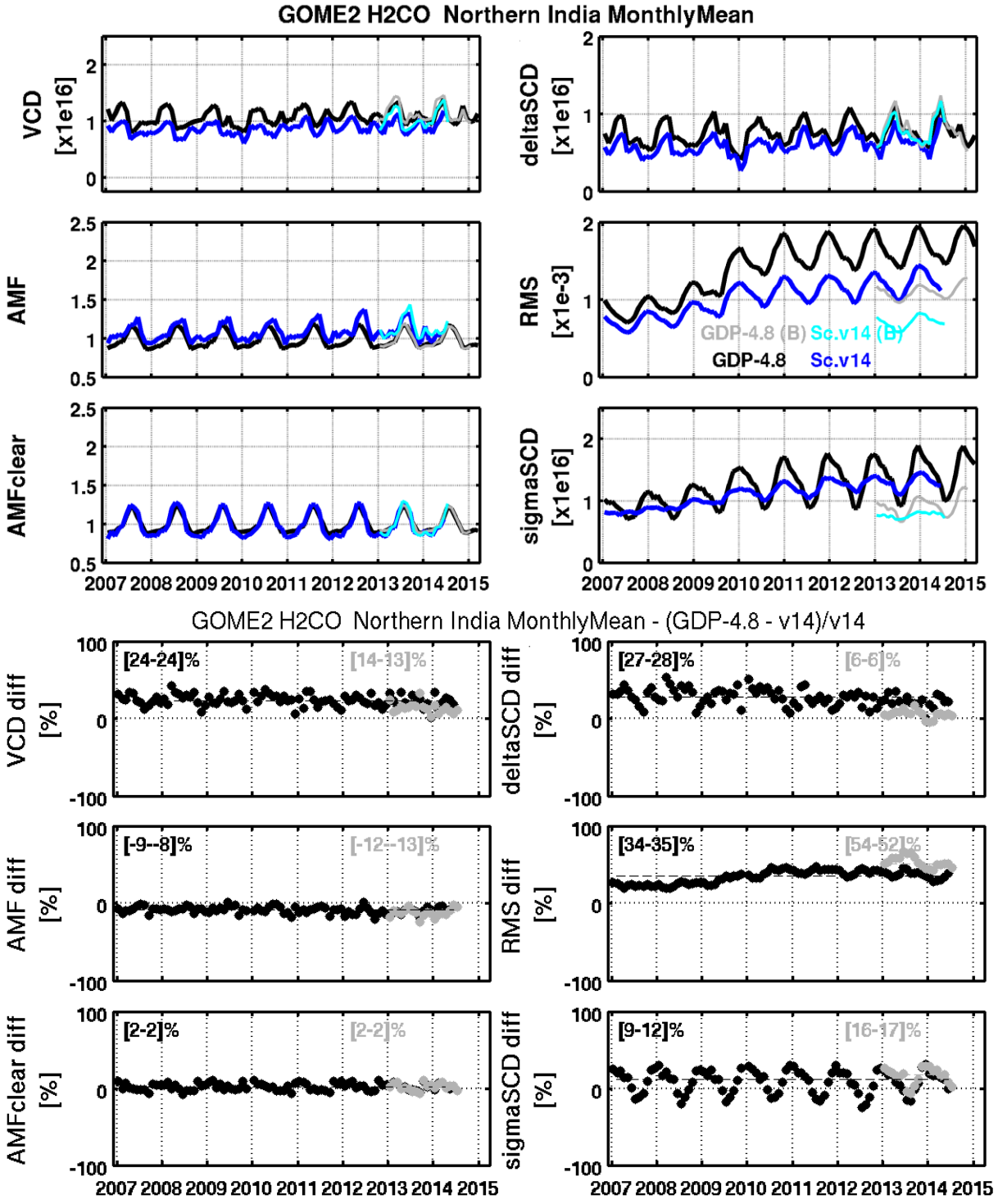

Figure 16: same as Figure 14, but for the India region.

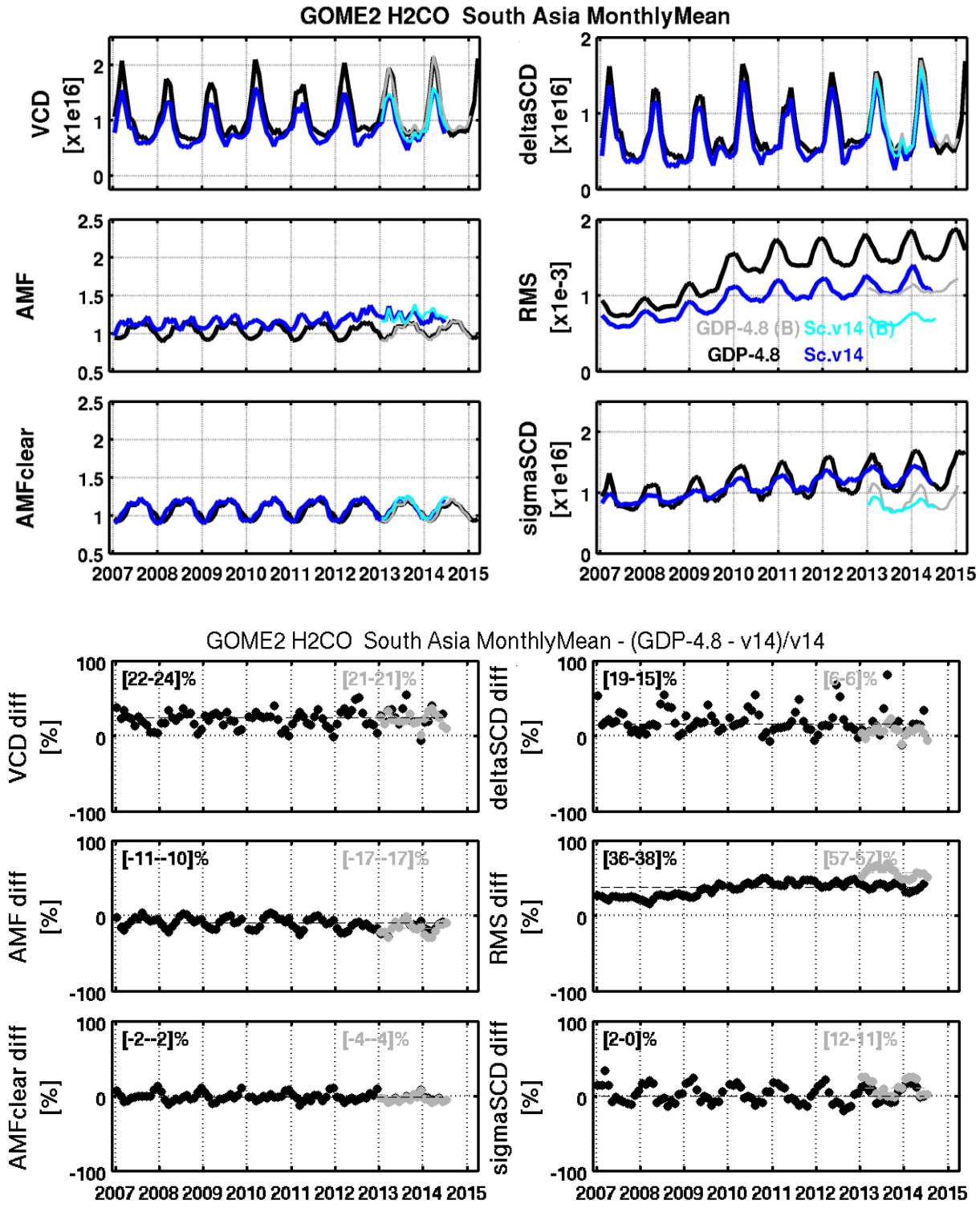

Figure 17: same as Figure 14, but for the South Asia region.

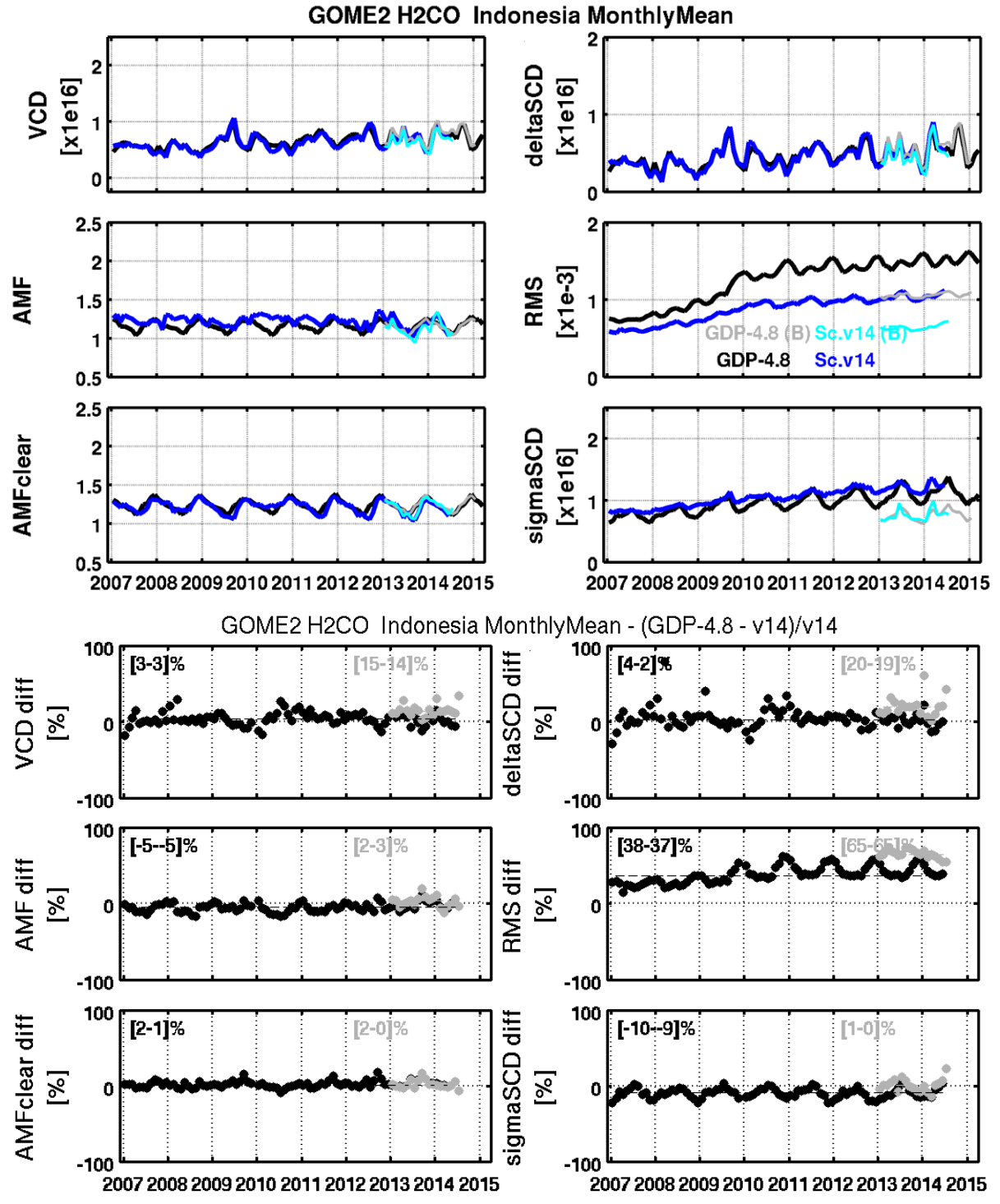

Figure 18: same as Figure 14, but for the Indonesia region.

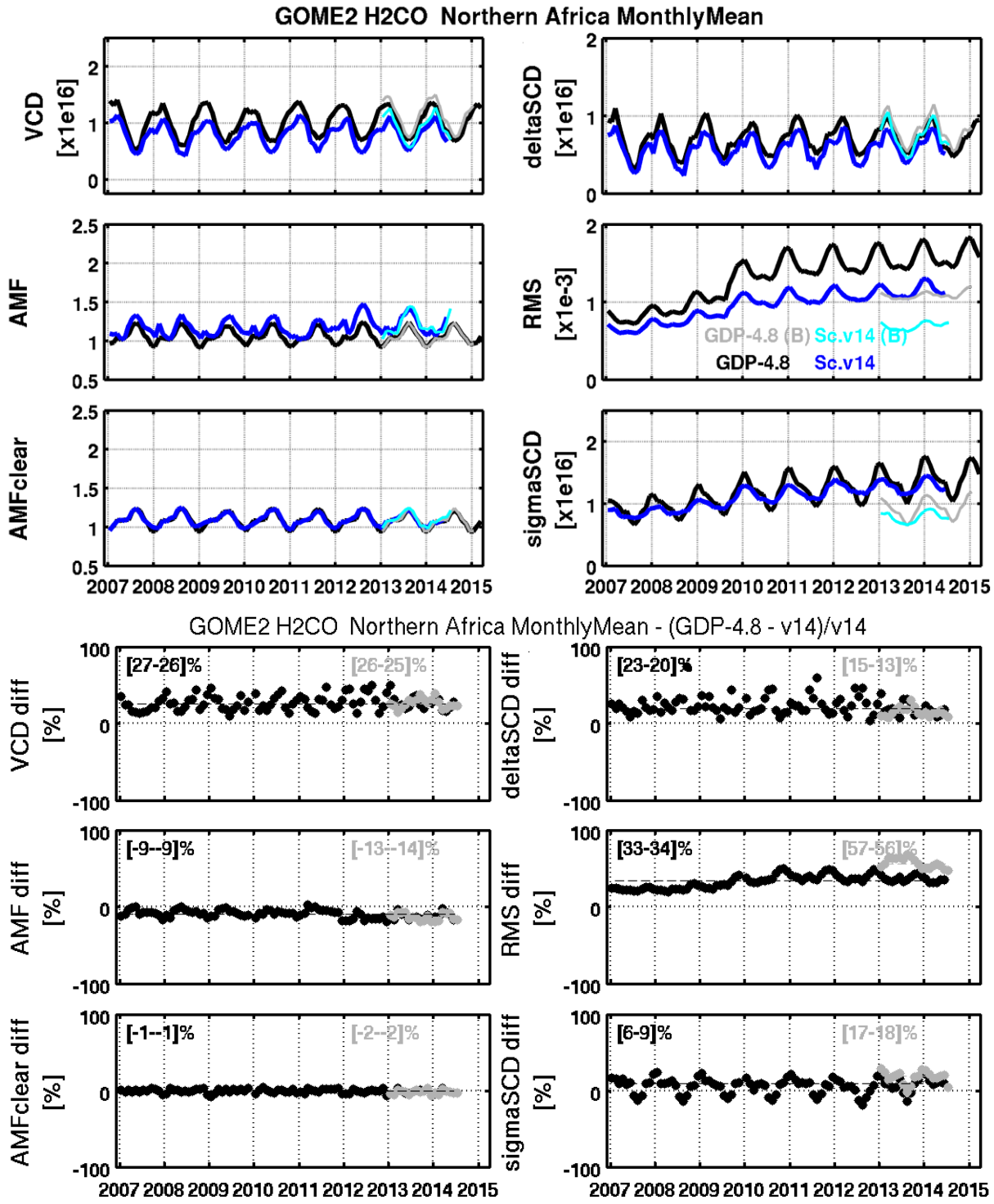

Figure 19: same as Figure 14, but for the Northern Africa region.

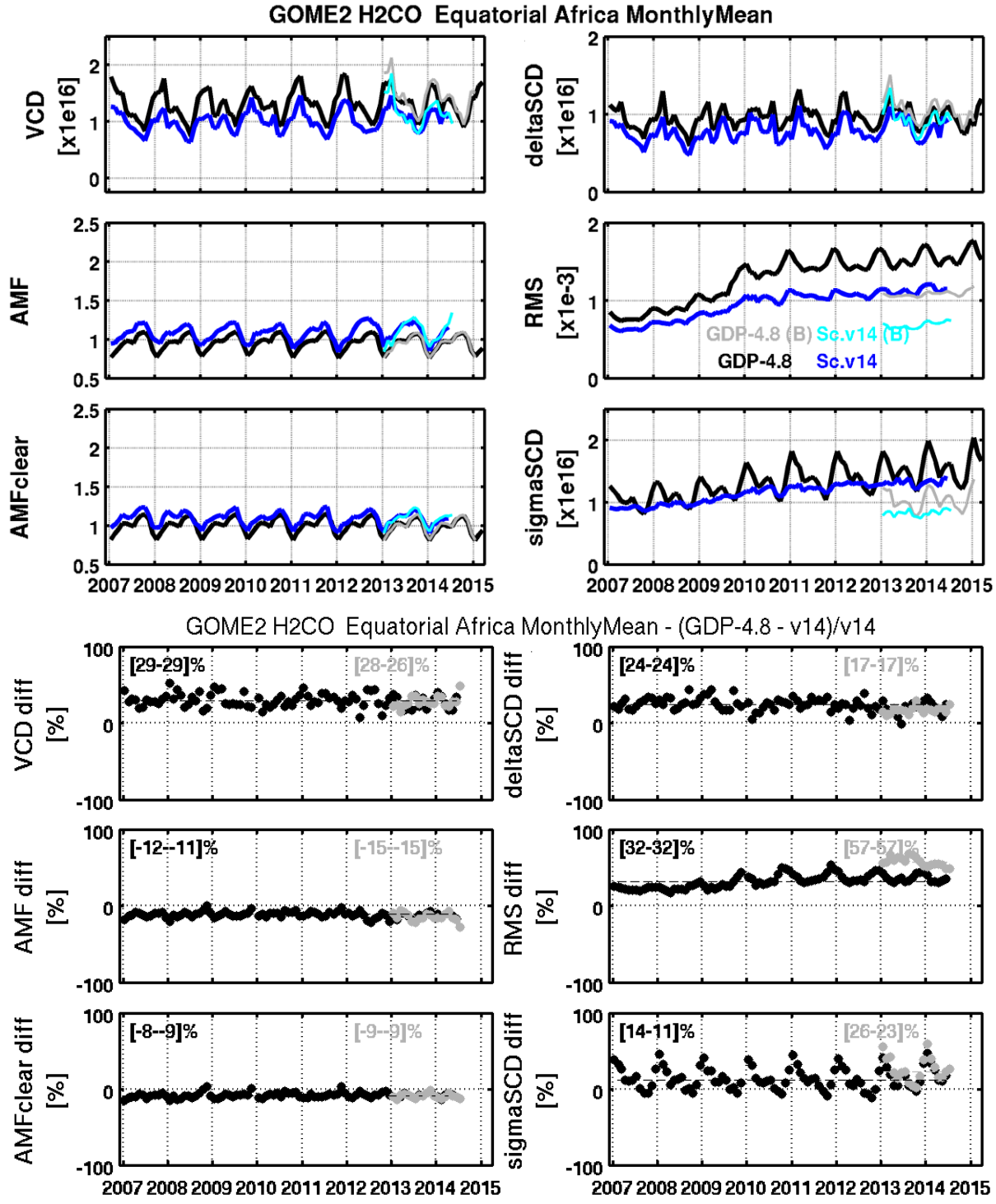

Figure 20: same as Figure 14, but for the Equatorial Africa region.

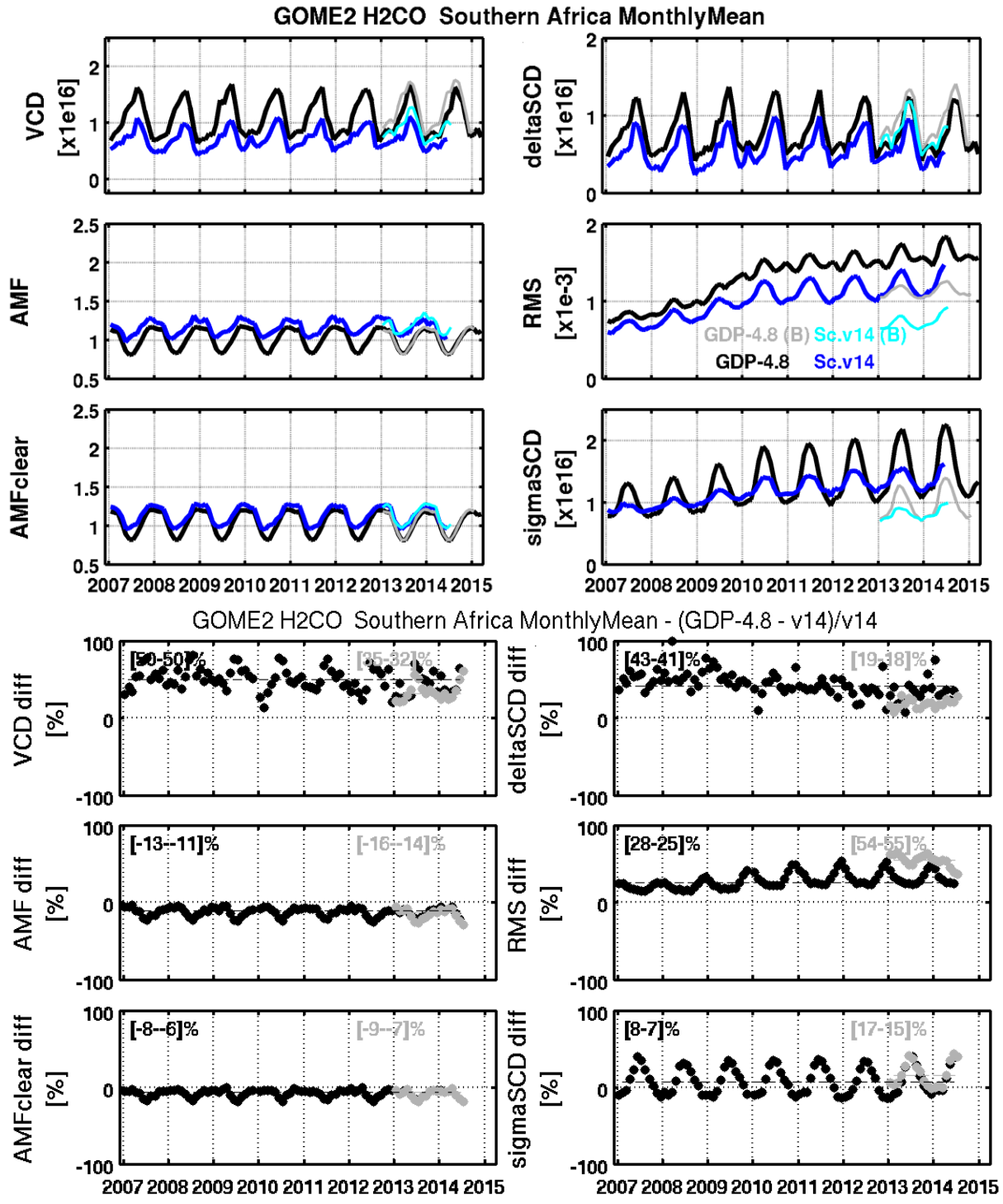

Figure 21: same as Figure 14, but for the Southern Africa regions.

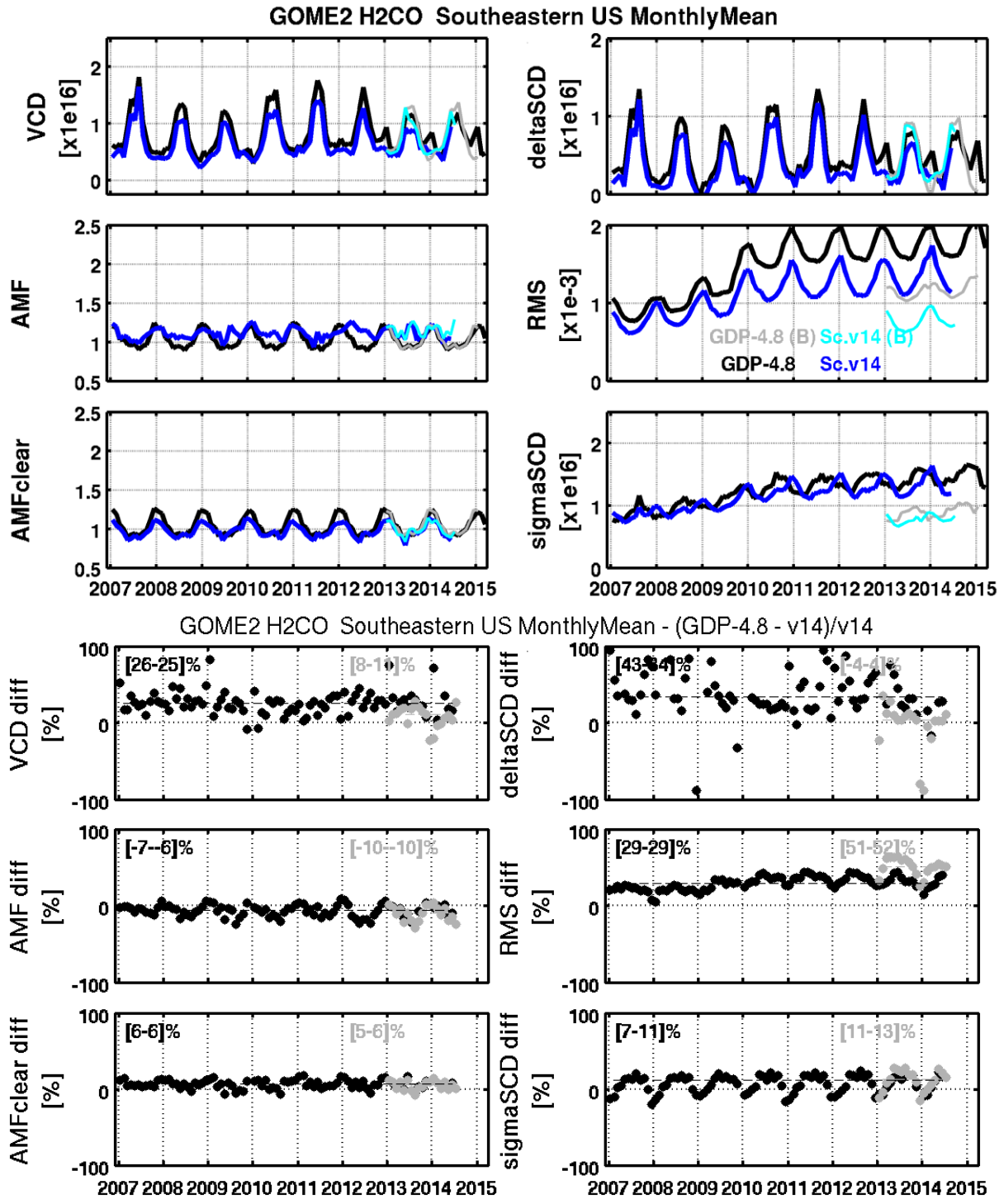

Figure 22: same as Figure 14, but for the Southeastern US region.

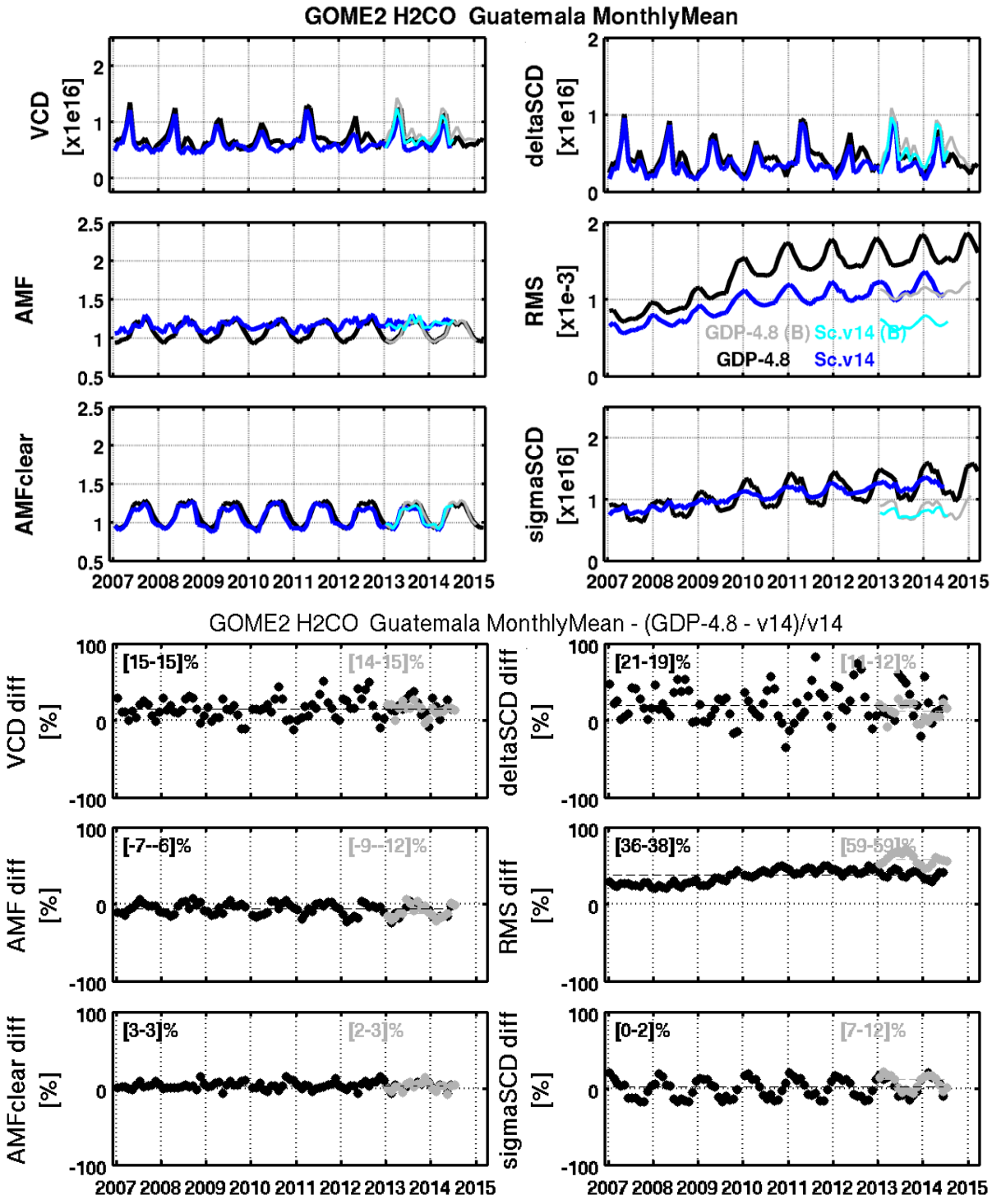

Figure 23: same as Figure 14, but for the Guatemala region.

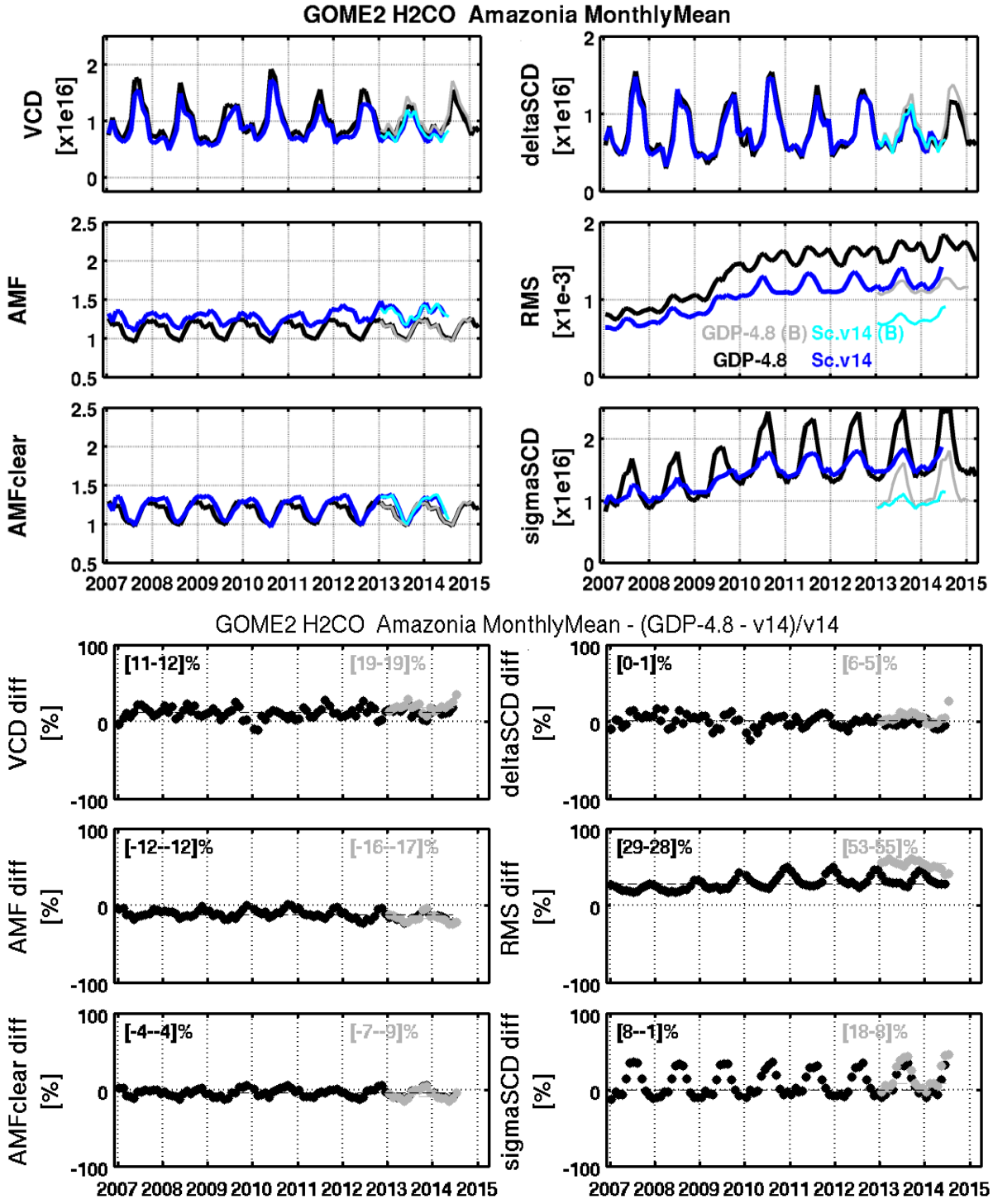

Figure 24: same as Figure 14, but for the Amazonia region.

- In both products, the HCHO VCD are generally very consistent between GOME-2A and GOME-2B. However, in some regions/months, GOME-2B HCHO VCDs are found to be slightly larger than those of GOME-2A (Australia, Africa, South Eastern US/summer time).
- The effect of GOME-2A degradation is visible both in the operational and in the scientific products.
- The GOME-2B standard deviations are comparable to those of GOME-2A at the beginning of the mission in both products.

- This is less the case of the RMS, which are somehow larger in GDP 4.8 for GOME-B retrievals than for GOME-2A at the beginning of the time series.
- The best agreement of the corrected slant columns is found in the Amazon and Indonesia regions (better than 10%), while the worse agreement is observed in Southern African region (40%). Generally, the GDP 4.8 HCHO dSCDs are larger than in the Sc.v14 product. Those differences are related to the inclusion of O_4 as an absorber in the fits in both intervals.
- Residuals are 30% (GOME-2A) to 60% (GOME-2B) larger in GDP 4.8. This is directly related to the use of remote radiance spectra as reference in the scientific algorithm.
- RMS increase slower in the scientific product, thanks to the fit of the instrumental slit function during the Fraunhofer wavelength calibration.
- Larger standard deviations are observed over the Amazon region. This could be improved by implementing an iterative spike removal algorithm.
- Clear-sky AMFs generally agree within 5% (surface albedo effect), except in equatorial and Southern Africa where differences reach 10% (surface altitude correction effect).
  Total AMFs are generally 10% to 20% lower in GDP 4.8 than in SC.v14. This systematic difference is related to the different cloud products (higher CTH in Rocinn v2.0 compared to Fresco v6).
- The relative impacts of O_4, cloud and albedo on the HCHO vertical columns are modulated depending on the particular situation of the different emission regions. The agreement between the two algorithms on the final HCHO VCD is generally within 15 to 25% for both instruments. The largest differences are observed over Southern Africa, where the different effects do not compensate.

F. COMPARISON WITH GROUND-BASED MAX-DOAS MEASUREMENTS

In this validation exercise, GOME-2A and B GDP 4.8 HCHO vertical column densities (VCDs) are compared to correlative observations from three MAX-DOAS instruments operated by BIRA-IASB and located at Xianghe (Beijing sub-urban area; 39.7°N, 117.0°E), Uccle (Belgium; 50.8°N, 4.3°E), and Bujumbura (Burundi; 3.0°S, 29.0°E). The periods covered by the ground-based data sets at these stations are 03/2010-03/2015, 04/2011-03/2015, and 11/2013-04/2014, respectively. Satellite HCHO VCD daily means are calculated using all pixels falling within a radius of 150 km around the stations and meeting the following selection criteria: HCHO slant column densities (SCDs) larger than $-4x10^{16}$ molec/cm^2, RMS lower than $3x10^{-3}$; solar zenith angle (SZA) lower than 70°, and cloud fraction lower than 40%. In order to allow direct comparison between GOME-2A and B and MAX-DOAS observations, the difference in vertical sensitivity between both measurement types should be taken into account. This can be done either by using the retrieved MAX-DOAS profile shapes as a priori for the calculation of satellite air mass factors or by applying the satellite column averaging kernels to the MAX-DOAS HCHO profiles. In this study, we choose the second way and the smoothed MAX-DOAS HCHO VCDs ($VCD_{MAXDOAS,smoothed}$) are derived for each day by averaging retrieved MAX-DOAS profiles falling within the daily satellite overpass time ± 1h and convolving the mean profile ($\mathbf{x}_{MAXDOAS}$) with the corresponding satellite column averaging kernel (AK_{sat}):

$$VCD_{MAXDOAS,smoothed} = AK_{sat} * \mathbf{x}_{MAXDOAS}$$

If the first altitude level of the satellite column averaging kernel is above the altitude of the station, then the averaging kernel is extrapolated down to the altitude of the station. MAX-DOAS profiles are retrieved by using the bePRO Optimal Estimation-based profiling tool (Clémer et al., 2010; Hendrick et al., 2014). Further information on the MAX-DOAS profile retrieval can be found in Vlemmix et al. (2015) and De Smedt et al. (2015). It should be noted that for all stations, MAX-DOAS observations in presence of optically thick clouds are excluded using the multiple-scattering cloud filter described in Gielen et al. (2014) since such sky conditions can potentially degrade the quality of the MAX-DOAS retrievals.

Comparison results (HCHO VCD time-series and corresponding scatterplots) are shown in Figure 25 and Figure 26 for Xianghe, in Figure 27 and Figure 28 for Uccle, and in Figure 29 for Bujumbura. For the latter station, scatterplots are not included due to the poorer statistics. Mean bias values are summarized in Table 5.

Table 5: Summary of the mean biases (in 10^{16} molec/cm^2) between GOME-2A and B and smoothed and unsmoothed MAX-DOAS HCHO VCDs. The values between brackets correspond to the mean relative biases.

		GOME-2A	GOME-2A over GOME-2B time period	GOME-2B
XIANGHE (39.7°N, 117.0°E) 03/2010-03/2015 for GOME-2A 12/2012-03/2015 for GOME-2B	**Unsmoothed MD**	**-0.68 ± 0.26 (-45 ± 13)**	**-0.73 ± 0.33 (-46 ± 11)**	**-0.76 ± 0.29 (-51 ± 20)**
	Smoothed MD	**0.09 ± 0.21 (13 ± 29)**	**0.09 ± 0.17 (11 ± 25)**	**0.02 ± 0.23 (3 ± 34)**
UCCLE (50.8°N, 4.3°E) 04/2011-03/2015 for GOME-2A 12/2012-03/2015 for GOME-2B	**Unsmoothed MD**	**-0.01 ± 0.24 (-2 ± 45)**	**-0.04 ± 0.24 (-6 ± 42)**	**-0.12 ± 0.20 (-19 ± 37)**
	Smoothed MD	**0.07 ± 0.27 (13 ± 76)**	**0.04 ± 0.26 (7 ± 73)**	**-0.02 ± 0.24 (-4 ± 43)**
BUJUMBURA (3.0°S, 29.0°E) 12/2013-04/2014 for GOME-2A & B	**Unsmoothed MD**		**-0.55 ± 0.24 (-46 ± 18)**	**-0.33 ± 0.14 (-29 ± 11)**
	Smoothed MD		**-0.04 ± 0.25 (-5 ± 37)**	**0.22 ± 0.14 (38 ± 25)**

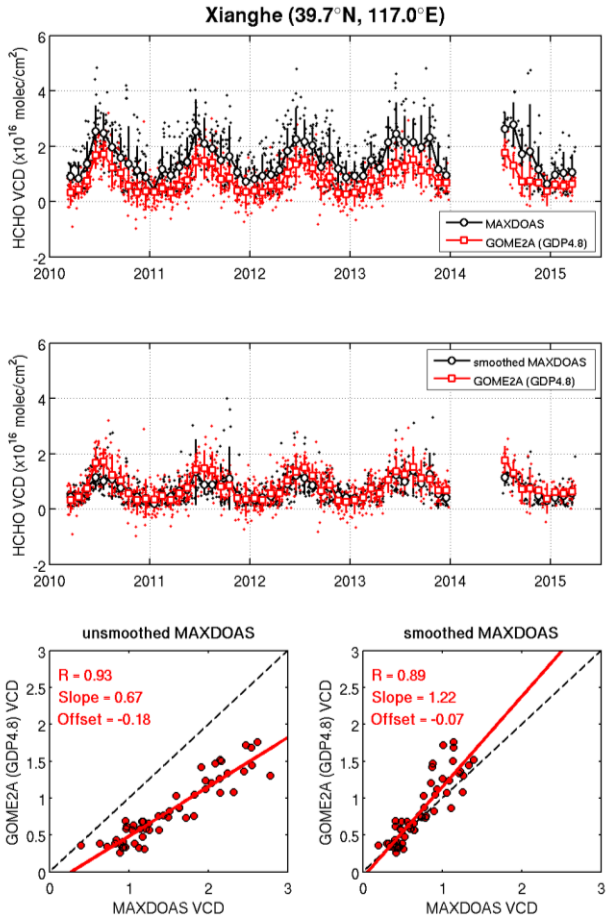

Figure 25: Comparison between GOME-2A and smoothed and unsmoothed MAX-DOAS HCHO VCDs at Xianghe. HCHO VCDs time-series appear in the upper (unsmoothed MAX-DOAS) and mid (smoothed MAX-DOAS) plots while the lower plots correspond to the scatterplots where VCDs are expressed in 10^{16} molec/cm^2. The gap between 01/2014 and 05/2014 in the time-series is due to a MAX-DOAS instrument failure.

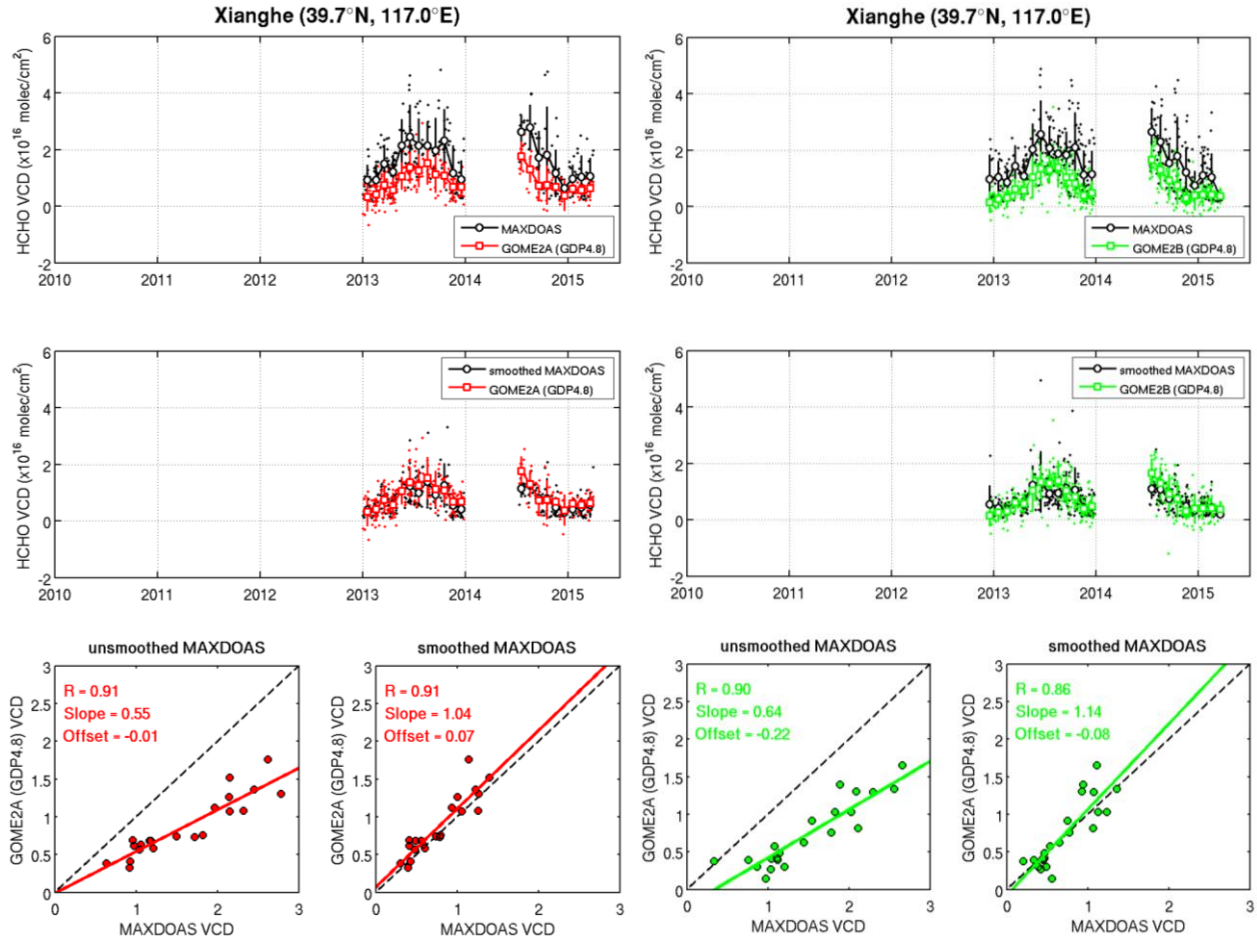

Figure 26: Left: Comparison between GOME-2A and smoothed and unsmoothed MAX-DOAS HCHO VCDs at Xianghe over the GOME-2B time period. Right: Comparison between GOME-2B and smoothed and unsmoothed MAX-DOAS HCHO VCDs at Xianghe. HCHO VCDs time-series appear in the upper (unsmoothed MAX-DOAS) and mid (smoothed MAX-DOAS) plots while the lower plots correspond to the scatterplots where VCDs are expressed in 10^{16} molec/cm^2. The gap between 01/2014 and 05/2014 in the time-series is due to a MAX-DOAS instrument failure.

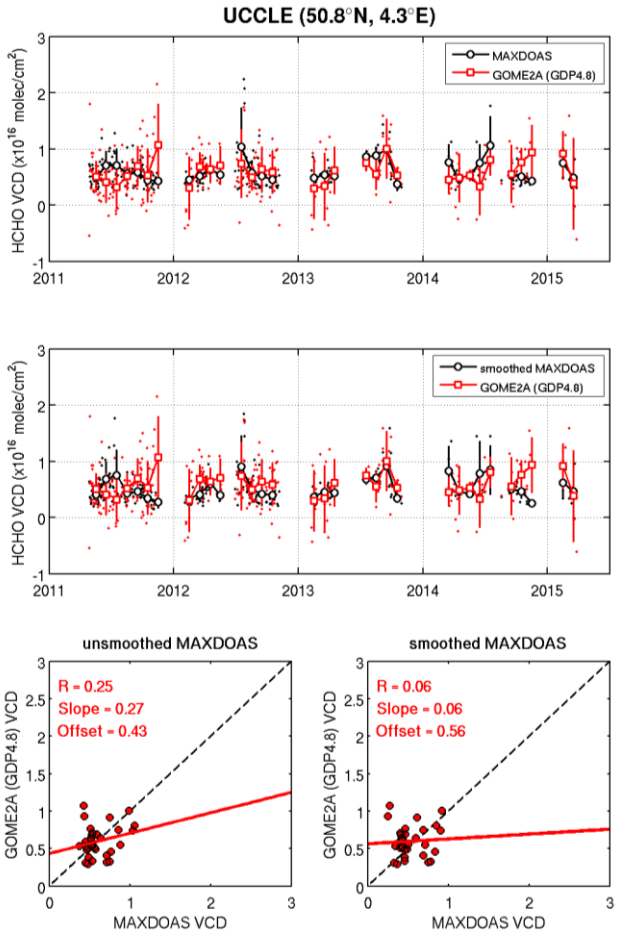

Figure 27: Comparison between GOME-2A and smoothed and unsmoothed MAX-DOAS HCHO VCDs at Uccle. HCHO VCDs time-series appear in the upper (unsmoothed MAX-DOAS) and mid (smoothed MAX-DOAS) plots while the lower plots correspond to the scatterplots where VCDs are expressed in 10^{16} molec/cm^2. The gaps in summer in the time-series is due to miniDOAS instrument failures. Those in winter are related to the absence of MAX-DOAS retrievals passing the quality control due to the larger noise on the measurements during the winter period where lower HCHO VCD values are observed.

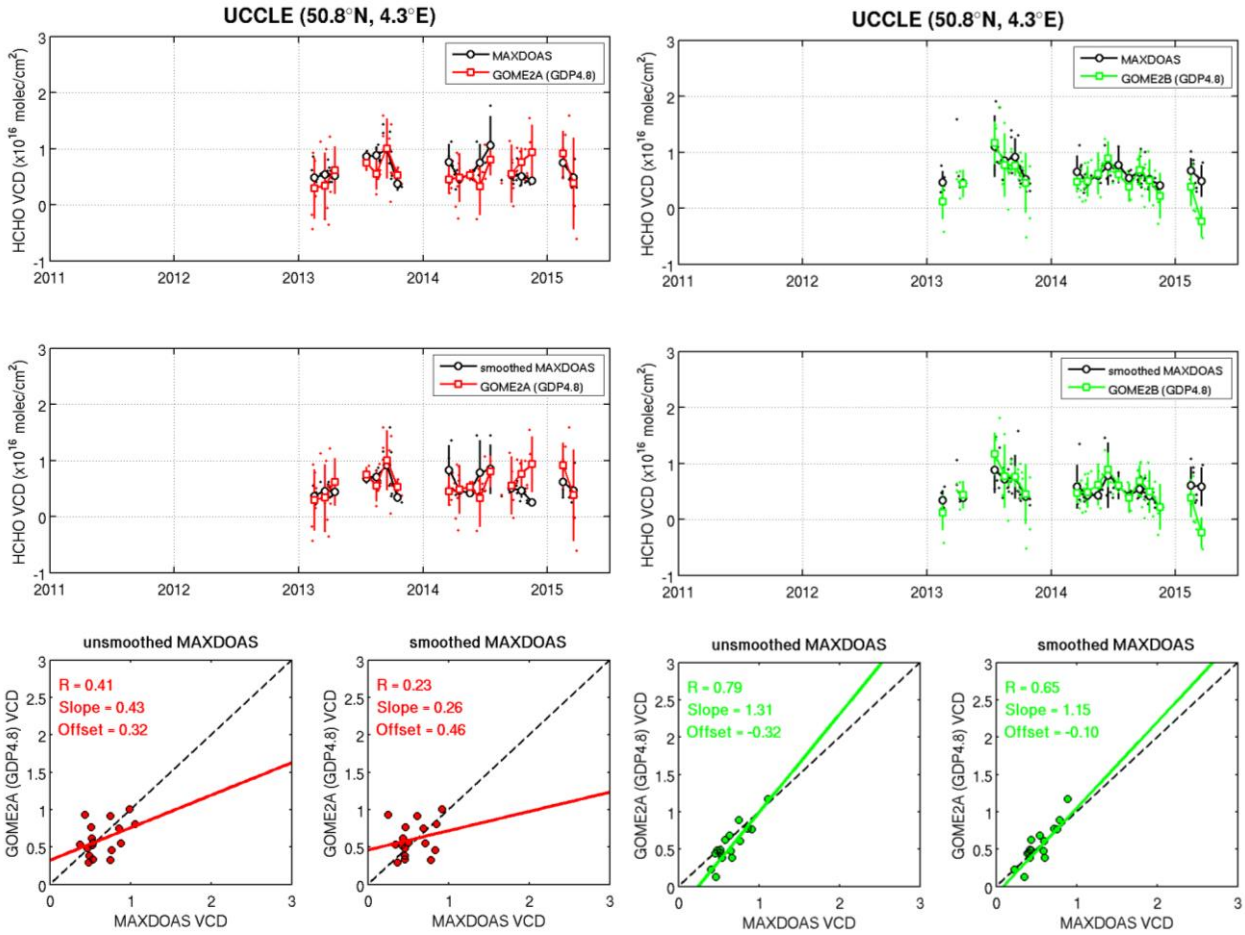

Figure 28: Left: Comparison between GOME-2A and smoothed and unsmoothed MAX-DOAS HCHO VCDs at Uccle over the GOME-2B time period. Right: Comparison between GOME-2B and smoothed and unsmoothed MAX-DOAS HCHO VCDs at Uccle. HCHO VCDs time-series appear in the upper (unsmoothed MAX-DOAS) and mid (smoothed MAX-DOAS) plots while the lower plots correspond to the scatterplots where VCDs are expressed in 10^{16} molec/cm^2. The gaps in summer in the time-series is due to miniDOAS instrument failures. Those in winter are related to the absence of MAX-DOAS retrievals passing the quality control due to the larger noise on the measurements during the winter period where lower HCHO VCD values are observed.

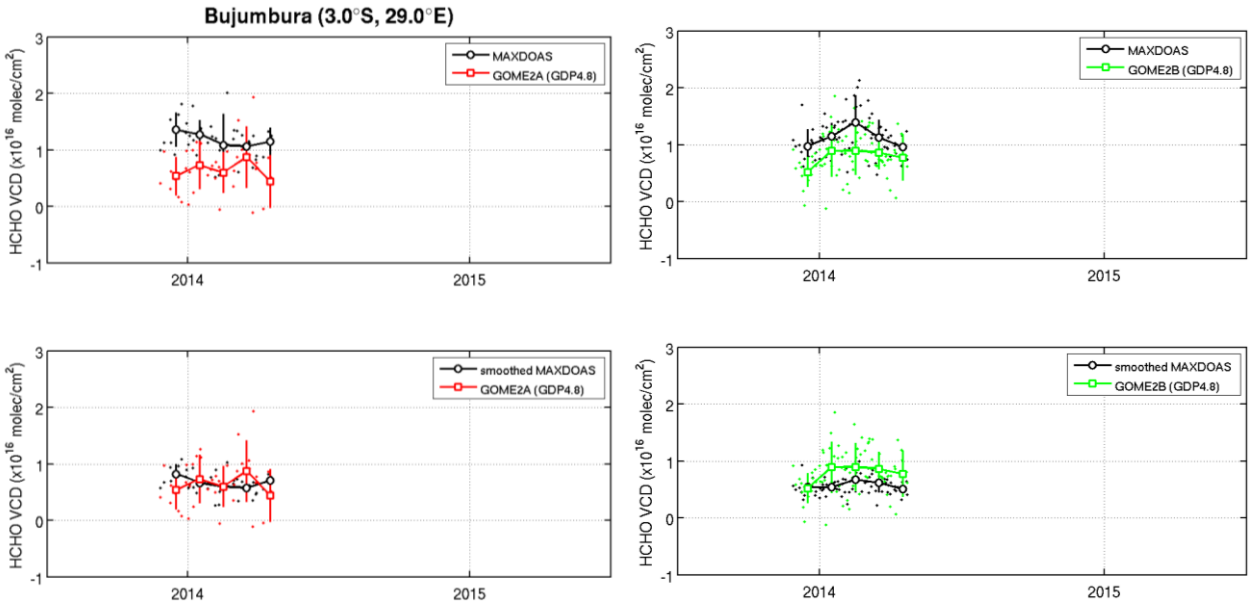

Figure 29: Comparison between GOME-2A (left) and B (right) and unsmoothed and smoothed MAX-DOAS HCHO VCDs at Bujumbura. The absence of comparison results after April 2014 is due to a failure in the UV channel of the MAX-DOAS instrument. The UV channel is working again since April 2015.

It can be seen from the scatter plots and Table 5 that the smoothing of the MAX-DOAS data significantly reduces the biases between GOME-2A and -B and MAX-DOAS data except for GOME-2A in Uccle. In contrast, the smoothing of the MAX-DOAS data does not improves the correlation between GOME-2A and -B and MAX-DOAS. Looking more in details at comparisons between GOME-2A and -B and smoothed MAX-DOAS HCHO VCDs, the following features are observed:

- Xianghe: Good agreement between GOME-2A and -B and MAX-DOAS in terms of correlation (~0.9) and slopes (1.04-1.22). The mean bias is lower for GOME-2B (0.02 x 10^{16} molec/cm^2) than for GOME-2A (0.09 x 10^{16} molec/cm^2).
- Uccle: Although mean bias values are reasonable (0.04-0.07 x 10^{16} molec/cm^2), a bad agreement is obtained between GOME-2A and MAX-DOAS in terms of correlation (<0.3) and slopes (<0.3). A significantly better agreement is observed for GOME-2B (R=0.65, S=1.15, mean bias=-0.02 x 10^{16} molec/cm^2).
- Bujumbura: In contrast to the two other stations, the mean bias is lower for GOME-2A (-0.04 x 10^{16} molec/cm^2) than for GOME-2B (0.22 x 10^{16} molec/cm^2). These bias values indicate that GOME-2B is larger than GOME-2A at this station. This feature will be investigated and the comparison statistics will be improved by extending the data sets to year 2015.

G. CONCLUSIONS AND PERSPECTIVES

This document reports on the validation of the NRT, offline and reprocessed O3M-SAF GOME-2A and B HCHO column data products retrieved at DLR with versions 4.8 of the GOME Data Processor (GDP), using level-1B data based on the level-0-1B processor versions 5.3 and 6.0. HCHO column data are compared to scientific retrievals (version 14) using the same level 1 data.

The following main conclusions can be drawn:

1. Particular features of the scientific prototype algorithm have been successfully implemented in the UPAS operational processor GDP4.8. The use of two interlinked fitting windows allows for a noise reduction both for GOME-2 on MetOp-A and MetOp-B, respectively by about 17 to 26% at the beginning of the sensor lifetimes.
2. The cloud product has been improved in GDP 4.8 (Lutz et al., 2015), leading to cloud-corrected air mass factors more consistent with the cloud-free air mass factors.
3. GOME-2B GDP 4.8 HCHO retrievals are in good agreement with the scientific prototype algorithm (Sc.v14), taking into account their differences in retrieval settings. The relative impacts of the differences on the HCHO vertical columns are modulated depending on the particular situation of the different emission regions. The agreement between the two algorithms on the final HCHO VCD is generally within 15 to 25% for both instruments. The largest differences are observed over Southern Africa, where differences can reach 50% in the case of GOME-2A.
4. The provision of total column averaging kernels in the level-2 HCHO operational product is a clear improvement, allowing for meaningful validation exercise using ground-based MAX-DOAS profile measurements.
5. The results of comparisons with ground-based MAX-DOAS columns (unsmoothed and smoothed) in Xianghe, Uccle, and Bujumbura are very encouraging since a good overall agreement is obtained between GOME-2A and B and MAX-DOAS at the three stations, except for GOME-2A over Uccle and GOME-2B over Bujumbura where larger discrepancies are observed. The possible origin(s) of the latter will be investigated in the future.
6. Further improvement of the slant columns in a future version of the GDP could be obtained by including O_4 in the spectral fits, by using earthshine mean radiance spectra as DOAS reference instead of the daily irradiances, by implementing an iterative residual spike correction method, and by implementing correction methods for time-dependent slit function changes.
7. Further improvement of the background correction could be obtained by adding an east-west normalisation of the columns across the orbit.
8. Further improvement of the vertical columns could be obtained by updating the surface albedo database.

H. REFERENCES

H.1. Applicable documents

[ATBD] Algorithm Theoretical Basis Document for GOME-2 Total Column Products of Ozone, NO_2, BrO, SO_2, H_2O, HCHO and Cloud Properties (GDP 4.8 for O3M-SAF OTO and NTO), DLR/GOME-2/ATBD/01, Rev. 3/A, Valks, P., et al., March 2015.

[PUM] Product User Manual for GOME Total Column Products of Ozone, NO_2, BrO, SO_2, H_2O, HCHO and Cloud Properties, DLR/GOME/PUM/01, Rev. 3/A, Valks, P., et. al., 2015.

[PRD] Product Requirements Document, SAF/O3M/FMI/RQ/PRD/001/Rev. 1.7, D. Hovila, S. Hassinen, D. Loyola, P. Valks, J., S. Kiemle, O. Tuinder, H. Joench-Soerensen, F. Karcher, 2015.

[VIM] Joint Committee for Guides in Metrology (JCGM/WG 2) 200:2008 & ISO/IEC Guide 99-12:2007, International Vocabulary of Metrology – Basic and General Concepts and Associated Terms (VIM), http://www.bipm.org/en/publications/guides/vim.html

[GUM] Joint Committee for Guides in Metrology (JCGM/WG 1) 100:2008, Evaluation of measurement data – Guide to the expression of uncertainty in a measurement (GUM), http://www.bipm.org/utils/common/documents/jcgm/JCGM_100_2008_E.pdf

[QA4EO] A Quality Assurance framework for Earth Observation, established by the CEOS. It consists of ten distinct key guidelines linked through an overarching document (the QA4EO Guidelines Framework) and more community-specific QA4EO procedures, all available on http://qa4eo.org/documentation.html A short QA4EO "user" guide has been produced to provide background into QA4EO and how one would start implementing it (http://qa4eo.org/docs/QA4EO_guide.pdf)

[GEOSS] http://www.epa.gov/geoss/

[Copernicus] http://www.copernicus.eu/

H.2 Peer-reviewed papers

- Boersma, K. F., Eskes, H. J. and Brinksma, E. J.: Error analysis for tropospheric NO_2 retrieval from space, J. Geophys. Res., 109(D4), doi:10.1029/2003JD003962, 2004.
- Boersma, K. F., Eskes, H. J., Dirksen, R. J., van der A, R. J., Veefkind, J. P., Stammes, P., Huijnen, V., Kleipool, Q. L., Sneep, M., Claas, J., Leitão, J., et al.: An improved tropospheric NO2 column retrieval algorithm for the Ozone Monitoring Instrument, Atmos. Meas. Tech., 4(9), 2329-2388, doi:10.5194/amt-4-1905-2011, 2011.
- Bogumil, K., Orphal, J.,Homann, T., Voigt, S., Spietz, P., Fleischmann, O.C.,Vogel, A.,Hartmann, M., Bovensmann, H.,Frerick, J., and Burrows, J.P., Measurements of molecular absorption spectra with the SCIAMACHY pre-flight model: Instrument characterization and reference data for atmospheric remote sensing in the 230-2380 nm region, J. Photochem. Photobiol. A: Chem. 157, 167-184, 2003.

- Brion, J., et al.: Absorption spectra measurements for the ozone molecule in the 350-830 nm region, J. Atmos. Chem., 30, 291-299, 1998.
- Cai, Z., Liu, Y., Liu, X., Chance, K., Nowlan, C. R., Lang, R., Munro, R. and Suleiman, R.: Characterization and correction of Global Ozone Monitoring Experiment 2 ultraviolet measurements and application to ozone profile retrievals, J. Geophys. Res., 117(D7), D07305, doi:10.1029/2011JD017096, 2012.
- Chance, K. and Kurucz, R. L.: An improved high-resolution solar reference spectrum for earth's atmosphere measurements in the ultraviolet, visible, and near infrared, *J*. Quant. Spectrosc. Radiat. Transf., 111(9), 1289-1295, 2010.
- Clémer, K., Van Roozendael, M., Fayt, C., Hendrick, F., Hermans, C., Pinardi, G., Spurr, R., Wang, P., and De Mazière, M., Multiple wavelength retrieval of tropospheric aerosol optical properties from MAXDOAS measurements in Beijing, Atmos. Meas. Tech., 3, 863-878, doi:10.5194/amt-3-863-2010, 2010.
- De Smedt, I., Müller, J.-F., Stavrakou, T., van der A, R., Eskes, H. and Van Roozendael, M.: Twelve years of global observations of formaldehyde in the troposphere using GOME and SCIAMACHY sensors, Atmos. Chem. Phys., 8(16), 4947-4963, 2008.
- De Smedt, I., Stavrakou, T., Müller, J. F., van Der A, R. J. and Van Roozendael, M.: Trend detection in satellite observations of formaldehyde tropospheric columns, Geophys. Res. Lett., 37(18), L18808, doi:10.1029/2010GL044245, 2010.
- De Smedt, I., Long-Term Global Observations of Tropospheric Formaldehyde Retrieved from Spaceborne Nadir UV Sensors, Ph.D. thesis, Faculty of Applied Sciences, University of Brussels, Belgium, 2011.
- De Smedt, I., Van Roozendael, M., Stavrakou, T., Müller, J.-F., Lerot, C., Theys, N., Valks, P., Hao, N. and van der A, R. J.: Improved retrieval of global tropospheric formaldehyde columns from GOME-2/MetOp-A addressing noise reduction and instrumental degradation issues, Atmos. Meas. Tech., 5, 2933–2949, doi:10.5194/amt-5-2933-2012, 2012.
- De Smedt, I., Stavrakou, T., Hendrick, F., Danckaert, T., Vlemmix, T., Pinardi, G., Theys, N., Lerot, C., Gielen, C., Vigouroux, C., Hermans, C., et al.: Diurnal, seasonal and long-term variations of global formaldehyde columns inferred from combined OMI and GOME-2 observations, Atmos. Chem. Phys. Discuss., 15(8), 12241–12300, doi:10.5194/acpd-15-12241-2015, 2015.
- Fleischmann, O. C., et al. : New ultraviolet absorption cross-sections of BrO at atmospheric temperatures measured by time-windowing Fourier transform spectroscopy, J. Photochem. Photobiol. A, 168, 117–132, 2004.
- Kleipool, Q. L., Dobber, M. R., de Haan, J. F. and Levelt, P. F.: Earth surface reflectance climatology from 3 years of OMI data, J. Geophys. Res., 113(D18), D18308, doi:10.1029/2008JD010290, 2008.
- Gielen, C., Van Roozendael, M., Hendrick, F., Pinardi, G., Vlemmix, T., De Bock, V., De Backer, H., Fayt, C., Hermans, C., Gillotay, D., and Wang, P.: A simple and versatile cloud-screening method for MAX-DOAS retrievals, Atmos. Meas. Tech. Discuss., 7, 5883-5920, doi:10.5194/amtd-7-5883-2014, 2014
- Hendrick, F., Müller, J.-F., Clémer, K., Wang, P., Mazière, M. D., Fayt, C., Gielen, C., Hermans, C., Ma, J., Pinardi, G., Stavrakou, T., Vlemmix, T., and Van Roozendael, M.: Four years of ground-based MAX-DOAS observations of HONO and NO2 in the Beijing area, Atmos. Chem. Phys., 14, 765-781, 2014.
- Koelemeijer, R. B. A., Stammes, P., Hovenier, J. W. and de Haan, J. F.: A fast method for retrieval of cloud parameters using oxygen A band measurements from the Global Ozone Monitoring Experiment, J. Geophys. Res., 106(D4), 3475-3490, doi:10.1029/2000JD900657 2001.
- Koelemeijer, R. B. A., de Haan, L. H. and Stammes, P.: A database of spectral surface reflectivity in the range 335 – 772 nm derived from 5 years of GOME observations, J. Geophys. Res., 108(D2), doi:10.1029/2002JD002429, 2003.
- Kurosu, T. P., OMHCHO README FILE, http://www.cfa.harvard.edu/_tkurosu/SatelliteInstruments/ OMI/PGEReleases/READMEs/OMHCHO_README.pdf, 2008.

- Lutz, R., D. Loyola, S. Gimeno Garcia, and F. Romahn, OCRA radiometric cloud fractions for GOME-2A/B, Atmos. Meas. Tech., to be submitted, 2015.
- Meller, R., and Moortgat, G. K.: Temperature dependence of the absorption cross section of HCHO between 223 and 323K in the wavelength range 225–375 nm, J. Geophys. Res., 105(D6), 7089–7102, doi:10.1029/1999JD901074, 2000.
- Palmer, P. I., Jacob, D. J., Chance, K. V., Martin, R. V., D, R. J., Kurosu, T. P., Bey, I., Yantosca, R. and Fiore, A.: Air mass factor formulation for spectroscopic measurements from satellites: Application to formaldehyde retrievals from the Global Ozone Monitoring Experiment, J. Geophys. Res., 106(D13), 14539-14550, doi:10.1029/2000JD900772, 2001.
- Platt, U. and Stutz, J.: Differential Optical Absorption Spectroscopy: Principles and Applications (Physics of Earth and Space Environments), Springer-Verlag, Berlin, Heidelberg, ISBN 978-3540211938, 2008.
- Puķīte, J., Kühl, S., Deutschmann, T., Platt, U. and Wagner, T.: Extending differential optical absorption spectroscopy for limb measurements in the UV, Atmos. Meas. Tech., 3(3), 631-653, doi:10.5194/amt-3-631-2010, 2010.
- Richter, A., Begoin, M., Hilboll, A. and Burrows, J. P.: An improved NO2 retrieval for the GOME-2 satellite instrument, Atmos. Meas. Tech., 4(6), 213-246, doi:10.5194/amt-4-1147-2011, 2011.
- Rozanov, A., Rozanov, V., and Burrows, J. P.: A numerical radiative transfer model for a spherical planetary atmosphere: Combined differential integral approach involving the Piccard iterative approximation, J. Quant. Spectrosc. Radiat. Transfer, 69, 491–512, 2001.
- Spurr, R. J. D.: Linearized radiative transfer theory, A general discrete ordinate approach to the calculation of radiances and analytic weighting functions, with applications to atmospheric remote sensing, Thesis Manuscript, Technische Universiteit Eindhoven, 2001.
- Spurr, R. J. D.: LIDORT and VLIDORT: Linearized pseudo-spherical scalar and vector discrete ordinate radiative transfer models for use in remote sensing retrieval problems, in Light Scattering Reviews, edited by A. Kokhanovsky, pp. 229–271, Berlin, 2008.
- Valks, P., Pinardi, G., Richter, A., Lambert, J.-C., Hao, N., Loyola, D., Van Roozendael, M. and Emmadi, S.: Operational total and tropospheric NO2 column retrieval for GOME-2, Atmos. Meas. Tech., 4(7), 1491-1514, doi:10.5194/amt-4-1491-2011, 2011.
- Vandaele, A.C., et al.: High-resolution Fourier transform measurement of the NO_2 visible and near-infrared absorption cross-section: Temperature and pressure effects, J. Geophys. Res., 107, D18, 4348, doi:10.1029/2001JD000971, 2002.
- Veefkind, J. P., Aben, I., McMullan, K., Förster, H., de Vries, J., Otter, G., Claas, J., Eskes, H. J., de Haan, J. F., Kleipool, Q., van Weele, M., et al.: TROPOMI on the ESA Sentinel-5 Precursor: A GMES mission for global observations of the atmospheric composition for climate, air quality and ozone layer applications, Remote Sensing of Environment, 120(0), 70-83, 2012.
- Vlemmix, T., F. Hendrick, G. Pinardi, I. De Smedt, C. Fayt, C. Hermans, A. Piters, P. Levelt, and M. Van Roozendael, MAX-DOAS observations of aerosols, formaldehyde and nitrogen dioxide in the Beijing area: comparison of two profile retrieval approaches, Atmospheric Measurement Techniques, 8, 941-963, 2015.
- Vountas, M., Rozanov, V. V. and Burrows, J. P.: Ring effect: impact of rotational Raman scattering on radiative transfer in earth's atmosphere, J. of Quant. Spec. and Rad. Trans., 60(6), 943-961, 1998.
- Wang, P., Stammes, P., van der A, R., Pinardi, G., and Van Roozendael, M.: FRESCO+: an improved O_2 A-band cloud retrieval algorithm for tropospheric trace gas retrievals, Atmos. Chem. Phys., 8, 6565-6576, doi:10.5194/acp-8-6565-2008, 2008.
- Zhou, Y., Brunner, D., Boersma, K. F., Dirksen, R. and Wang, P.: An improved tropospheric NO2 retrieval for OMI observations in the vicinity of mountainous terrain, Atmos. Meas. Tech., 2(2), 401-416, 2009

H.3 Technical notes

- O3-SAF validation Report, Offline Total Formaldehyde (O3M-10 OTO HCHO) GOME-2, H2CO, 2010.
- O3-SAF validation Report, Offline Total Formaldehyde (O3M-58 OTO HCHO) GOME-2, H2CO, 2013.
- De Smedt, I., T. Stavrakou, J.-F. Müller, N. Hao, et al., H_2CO columns retrieved from GOME-2: first scientific results and progress towards the development of an operational product, Proceedings of the 2009 EUMETSAT Meteorological Satellite Conference, Bath, U.K., 2009.
- Callies, J., Corpaccioli, E., Eisinger, M., Hahne, A., and Lefebvre, A.: GOME-2- Metop's second-generation sensor for operational ozone monitoring, ESA Bull., 102, 28–36, 2000.
- Dikty, S. and Richter, A.: GOME-2 on MetOp-A Support for Analysis of GOME-2 In-Orbit Degradation and Impacts on Level 2 Data Products, Final Report, Version 1.2 - Issue Date: 14.10.2011.
- Lacan, A. and Lang, R.: Investigation on GOME-2 throughput degradation, Final report, EUM/LEO/REP/09/0732 Issue 1.1, 16. July 2011.
- Lang, R., Munro, R., Livschitz, Y., Dyer, R., and Lacan, A.: GOME-2 FM3 Long-Term In-Orbit Degradation - Basic Signatures After 2nd Throughput Test, EUMETSAT Technical report, EUM.OPS-EPS.DOC.09.0464, 2009.
- Munro, R., Eisinger, M., Anderson, C., Callies, J., Corpaccioli, E., Lang, R., Lefebvre, A., Livschitz, Y., and Albinana, A. P.: GOME-2 on MetOp, Proc. of The 2006 EUMETSAT Meteorological Satellite Conference, Helsinki, Finland, 2006.
- Siddans et al.: Analysis of GOME-2 Slit function Measurements: Final Report Eumetsat Contract No. EUM/CO/04/1298/RM, 2006.